Experimental Liquidus Studies of the Pb-Fe-Si-O System in Equilibrium with Metallic Pb

M. SHEVCHENKO and E. JAK

Phase equilibria of the Pb-Fe-Si-O system have been investigated at 943 K to 1773 K (670 °C to 1500 °C) for oxide liquid in equilibrium with liquid Pb metal and solid oxide phases: (a) quartz, tridymite, or cristobalite; (b) (fayalite + tridymite) or (fayalite + spinel); (c) spinel (Fe_3O_4); (d) complex lead-iron silicates (melanotekite $PbO{\cdot}FeO_{1.5}{\cdot}SiO_2$, barysilite $8PbO{\cdot}FeO{\cdot}6SiO_2$, $5PbO{\cdot}FeO_{1.5}{\cdot}SiO_2$, and $6PbO{\cdot}FeO_{1.5}{\cdot}SiO_2$); (e) lead silicates ($Pb_2SiO_4$, $Pb_{11}Si_3O_{17}$); (f) lead ferrites (magnetoplumbite $Pb_{1+x}Fe_{12-x}O_{19-x}$ solid solution range); and (g) lead oxide (PbO, massicot). High-temperature equilibration on primary phase or iridium substrates, followed by quenching and direct measurement of Pb, Fe, and Si concentrations in the phases with the electron probe X-ray microanalysis, has been used to accurately characterize the system in equilibrium with Pb metal. All results are projected onto the PbO-"FeO"-SiO_2 plane for presentation purposes. The present study is the first systematic characterization of liquidus over a wide range of compositions in this system in equilibrium with metallic Pb.

https://doi.org/10.1007/s11663-017-1136-0

I. INTRODUCTION

THE chemical compositions of slags in typical lead smelting operations can be represented by the Pb-Zn-Fe-Cu-Si-Ca-Al-Mg-O system. Accurate data on slag-solid-metal phase equilibria, activities of lead species in the slag, and partitioning of elements between gas, slag, metal, and solid phases are essential to support the further optimization and development of complex lead smelting, refining, and recycling processes.

The present experimental studies of gas-slag-metal-solid oxide phase equilibria in the Pb-Fe-Si-O low-order system are an important part of an integrated thermodynamic modeling and experimental research program for the above multicomponent system. Particular focus in this study has been given to resolving discrepancies between the previously reported data and providing new data for conditions not previously investigated in all slag systems containing iron oxide in equilibrium with metallic lead.

The earlier studies of the lead-containing slag systems[1–11] were focused on equilibria in air, with limited investigations[12] at most reducing conditions (equilibria with metallic iron), which have low PbO concentrations in the slag (<1 wt pct PbO). No studies have been reported on phase equilibria in the Pb-Fe-Si-O system in equilibrium with metallic lead over wide ranges of temperatures, compositions, and phase fields. Several experimental[13–19] and modeling[20] studies were undertaken on the Pb-Fe-Ca-Si-O system at lead blast furnace conditions; none of them reported any results on the slag liquidus. Only one study[21] was found on the Pb-Fe-Si-O slag in equilibrium with Pb metal, limited to a single 1473 K (1200 °C) isotherm at tridymite saturation. Glasser[22] examined a subsolidus isothermal section of the PbO-"Fe_2O_3"-SiO_2 system in air at 923 K (650 °C). Some information on the liquidus surface in air can also be derived from the work by Nitta.[23] Some studies on the solid-liquid equilibria in the PbO-"Fe_2O_3"-SiO_2 system in air have been performed using the equilibration/quenching/microanalysis technique.[24] The information available at that time was used for thermodynamic modeling[25] to estimate the phase equilibria at metallic lead saturation based on the results at different conditions (liquidus in air[24] and at metallic iron saturation[12]). Accurate thermodynamic predictions require experimental data on all low-order systems (binary and ternary) and all phases that can be formed. Significant gaps in experimental data on the Pb-Zn-Fe-Cu-Si-Ca-Al-Mg-O system have been identified to be essential for revision of the current thermodynamic database.[25,26]

According to the current public FactSage 6.2 database,[25,26] most of the liquidus surface in the PbO-"FeO"-SiO_2 system in equilibrium with Pb metal is described by the quartz, tridymite, cristobalite (SiO_2),

M. SHEVCHENKO and E. JAK are with the Pyrometallurgy Innovation Centre (PYROSEARCH), The University of Queensland, Brisbane, QLD 4072, Australia. Contact e-mail: m.shevchenko@uq.edu.au

Manuscript submitted May 11, 2017.
Article published online November 22, 2017.

and spinel (Fe_3O_4) primary phase fields. Liquid immiscibility was expected at very high temperatures [> 1873 K (1600 °C)] over the cristobalite liquidus field. Other predicted primary phase fields were fayalite (Fe_2SiO_4), wustite (FeO_{1+x}), melanotekite ($PbO{\cdot}FeO_{1.5}{\cdot}SiO_2$), melilite (range of solid solutions between $2PbO{\cdot}FeO{\cdot}2SiO_2$ and $2PbO{\cdot}Fe_2O_3{\cdot}SiO_2$), $5PbO{\cdot}FeO_{1.5}{\cdot}SiO_2$, lead silicates (alamosite $PbSiO_3$, lead orthosilicate Pb_2SiO_4, and 4-lead silicate Pb_4SiO_6), lead ferrites (1:1 lead ferrite $PbO{\cdot}FeO_{1.5}$, plumboferrite $PbO{\cdot}4FeO_{1.5}$, magnetoplumbite $PbO{\cdot}10FeO_{1.5}$), and lead oxide (massicot, PbO). However, the exact extents of these phase fields are unknown. The current study focuses on the equilibria of the slag-(solid oxide)-(liquid Pb) phases over wide range of temperatures [923 K to 1773 K (670 °C to 1500 °C)] and compositions.

II. EXPERIMENTAL TECHNIQUE AND PROCEDURE

A. *Experimental Procedure and Sample Examination*

The experimental procedure and apparatus have been described in detail in previous publications by PYROSEARCH.[11,27,28] Initial mixtures were made by mixing high-purity powders of Fe_2O_3 (99.945 wt pct purity), PbO (99.9 wt pct purity), SiO_2 (99.9 wt pct purity), supplied by Alfa Aesar, MA; and "FeO" (99.9 wt pct purity), supplied by Sigma Aldrich, MO. The reagent "FeO" was assumed to be $FeO_{1.05}$, because there is no stable phase of the exact FeO composition. Pb powder (99.95 wt pct purity; supplied by Sigma Aldrich, MO) was added 20 to 30 wt pct in excess of the mass of the oxide mixture to ensure metallic lead was present at the final equilibrium. Fe powder (99.998 wt pct purity, supplied by Alfa Aesar, MA) was used for selected experiments in equilibrium with metallic iron and for preparation of the fayalite master-slag.

The initial compositions of the mixtures were selected so that following the experiments one or more crystalline phases would be present in equilibrium with liquid slag. The volume fraction of solids in the final phase assemblage was targeted to be below 50 pct, and preferably about 10 pct, to achieve the best quenching. An iterative procedure involving preliminary experiments was often needed to achieve the targeted proportion of the phases for given final temperature and composition, since the exact liquidus coordinates were not initially known. Less than 0.5 g of mixture was used in each equilibration experiment.

Three types of substrates were used for equilibration, depending on the conditions:

1. Silica ampoules, sealed under vacuum, were used to stop evaporation of the volatile components (Pb, PbO) as well as oxidation of the sample by residual oxygen in the gas atmosphere. Open silica crucibles were used only when the quenching rates were critical (*e.g.*, near the tridymite-fayalite boundary).
2. Magnetite (spinel) baskets, prepared by heating a folded iron foil (99.5 wt pct purity Fe, 0.1 mm thickness, supplied by Sigma Aldrich, MO) in CO_2 at 1473 K (1200 °C) for 2 to 3 hours (the stoichiometry of Fe_3O_4 was checked gravimetrically), were used for the experiments where spinel was one of the primary phases: slag + spinel + Pb metal (+ other solid oxides).
3. Iridium L-shape plates (> 99.9 pct purity, provided by Furuya Metal, Tokyo, Japan) were used for equilibration of slags with Pb metal and solids other than spinel or silica polymorphs—*i.e.*, lead-iron silicates or PbO. Iridium is the only refractory metal stable against the combination of molten Pb and PbO,[29] though it cannot be used in oxidizing conditions without Pb metal, since it reacts as described by the equation Ir (s) + PbO (l) + O_2 (g) = $PbIrO_{3+x}$ (s).[30]

Fig. 1—Backscattered scanning electron micrographs of quenched slag in the PbO-"FeO"-SiO_2 system in equilibrium with one or two crystalline phases and metallic liquid Pb (or solid Fe). Asterisk (*) shows that Pb has coalesced to large drops, none of which are present in the given image, but are located elsewhere. (*a*) Liq + PbO + Pb; (*b*) Liq + PbO + Pb; (*c*) Liq + Tridymite + Pb + Fe(solid); (*d*) Liq + Spinel + Fayalite(F_2S) + Pb; (*e*) Liq + Melanotekite(PFS) + Barysilite(P_8FS_6) + Pb*; (*f*) Liq + Tridymite + Fayalite(F_2S) + Pb; (*g*) Liq + Spinel + Pb; (*h*) Liq + Melanotekite(PFS) + Barysilite (P_8FS_6) + Pb; (*i*) Liq + Spinel + Barysilite(P_8FS_6) + Pb; (*j*) Liq + Tridymite(SiO_2) + Pb; (*k*) Liq + Spinel + Pb; (*l*) Liq + P_2S + Barysilite(P_8FS_6) + Pb*; (*m*) Liq + P_6FS + Pb; (*n*) Liq + P_5FS + Magnetoplumbite($P_{1+x}F_{12-x}$) + Pb*.

All equilibration experiments were carried out in a vertical reaction tube (impervious recrystallized alumina, 30-mm inner diameter) within an electrical resistance-heated silicon carbide (SiC) furnace. A working thermocouple in a recrystallized alumina sheath was placed immediately next to the sample to monitor the actual sample temperature. The working thermocouple was periodically calibrated against a standard thermocouple (supplied by the National Measurement Institute of Australia, NSW, Australia). The overall absolute temperature accuracy of the experiments was estimated to be ± 3 K. An inert atmosphere of high-purity Argon gas (99.999 pct purity; supplied by Coregas, NSW, Australia) in a gas-tight system was used for all experiments.

The sample was suspended in the hot zone of the furnace by Kanthal support wire (0.7 or 1-mm diameter). Samples were pre-melted for various times (0.5 to 19 hours, see Table II) at 20 K to 200 K above the equilibration temperature, to form a homogeneous slag. This was followed by equilibration at the final target temperature and atmosphere condition for the required time (from 0.5 to 1 hour in tridymite and spinel primary phase fields at high temperatures to 3 to 5 days for quartz primary phase field at low temperature, see Table II). The primary phases were precipitated from the melts. For some experiments where the crystal precipitation from the viscous slag was slow, in particular, for lead and lead-iron silicates liquidus below 1073 K (800 °C), an extra pre-crystallization stage was introduced between the premelt and the final equilibration. To avoid undercooling, the sample was kept below the final temperature for several hours or days.

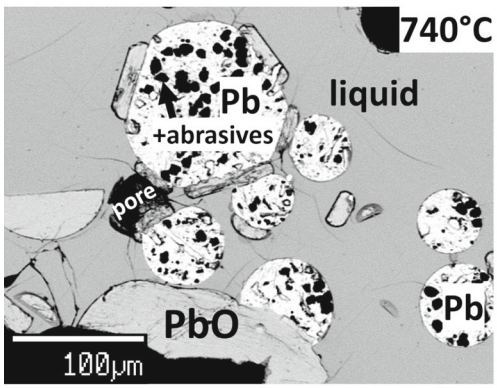

(a) Liq+PbO+Pb

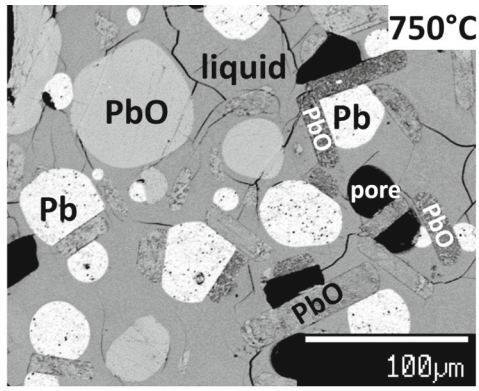

(b) Liq+PbO+Pb

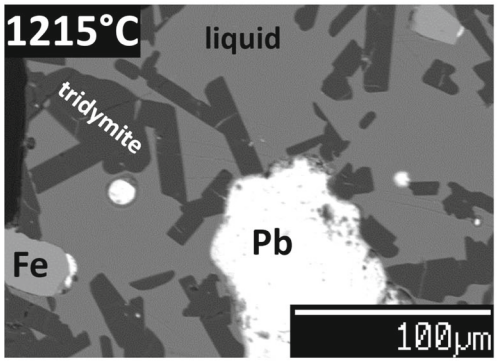

(c) Liq+Tridymite+Pb+Fe(solid)

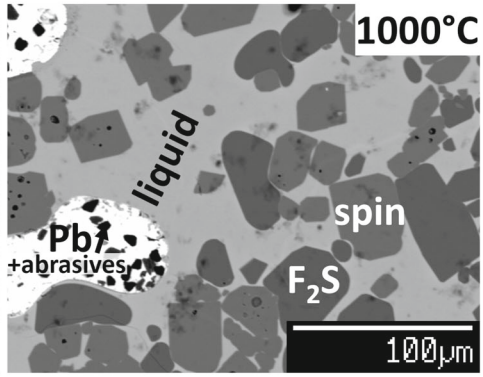

(d) Liq+Spinel+Fayalite(F_2S)+Pb

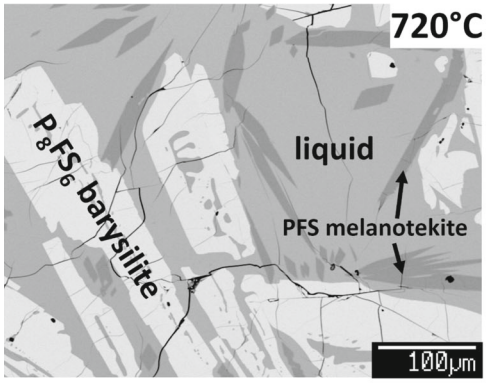

(e) Liq+Melanotekite+Barysilite+Pb*

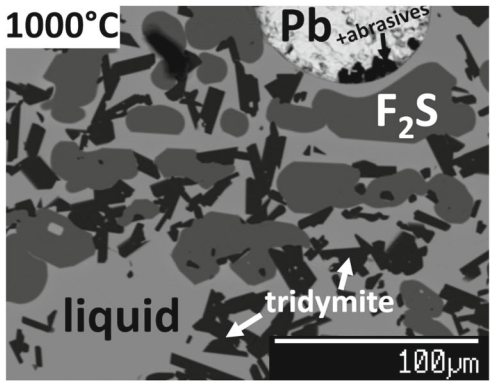

(f) Liq+Tridymite+Fayalite(F_2S)+Pb

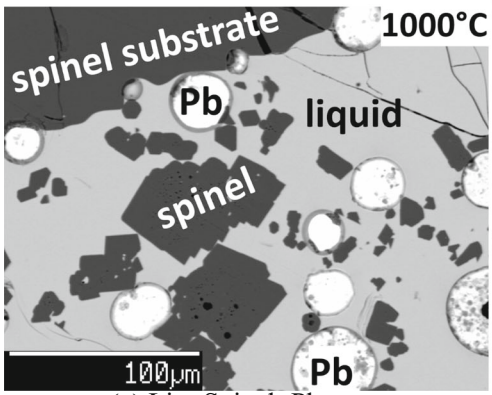

(g) Liq+Spinel+Pb

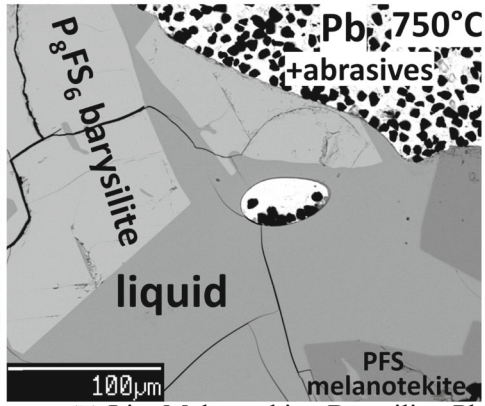

(h) Liq+Melanotekite+Barysilite+Pb

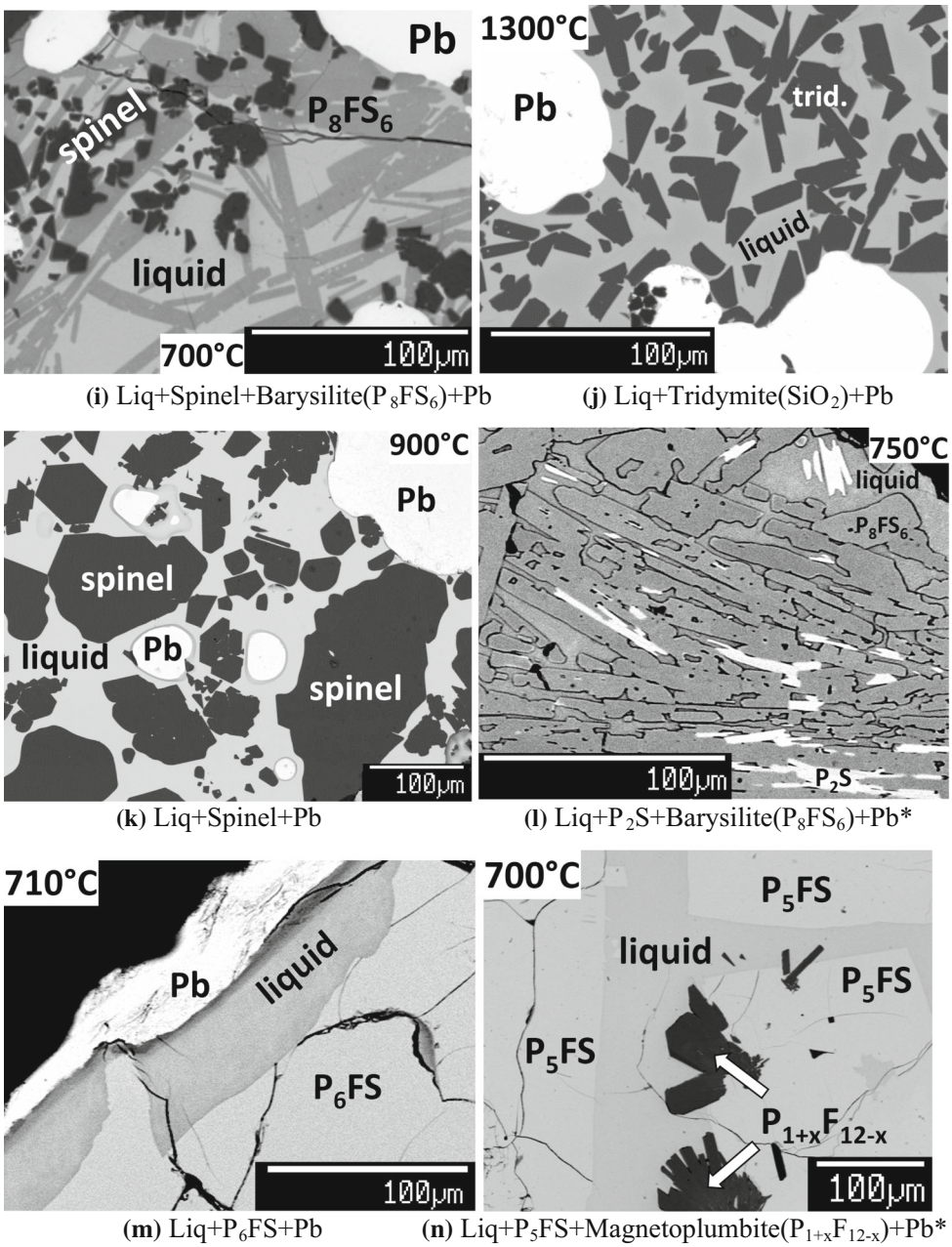

(i) Liq+Spinel+Barysilite(P_8FS_6)+Pb **(j)** Liq+Tridymite(SiO_2)+Pb

(k) Liq+Spinel+Pb **(l)** Liq+P_2S+Barysilite(P_8FS_6)+Pb*

(m) Liq+P_6FS+Pb **(n)** Liq+P_5FS+Magnetoplumbite($P_{1+x}F_{12-x}$)+Pb*

Fig. 1—continued.

At the end of the equilibration process, the sample was rapidly quenched in iced calcium chloride brine [< 255 K (−18 °C)]. The specimen was then washed thoroughly in water and ethanol before being dried on a hot plate, mounted in epoxy resin, and cross sections prepared using conventional metallographic polishing techniques.

The samples were examined by optical microscopy, carbon-coated, and the phase compositions were measured using an electron probe X-ray microanalysis technique with wavelength dispersive detectors (JEOL 8200L EPMA; Japan Electron Optics Ltd., Tokyo, Japan). The EPMA was operated with 15-kV accelerating voltage and 20 nA probe current using the Duncumb–Philibert atomic number, absorption, and fluorescence correction (ZAF correction). Hematite (Fe_2O_3), quartz (SiO_2), wollastonite ($CaSiO_3$) (supplied by Charles M. Taylor Co., Stanford, CA), and K-456 lead silicate glass (71 wt pct. PbO, supplied by NIST) standards were used for calibration of the EPMA. The concentrations of metal cations were measured with EPMA; no information on the different oxidation states of metal cations was obtained. Iron oxide concentrations were recalculated as FeO for presentation purposes. The molar ratios were used to avoid any ambiguity.

The ability to produce samples containing the primary phase solids and glassy or amorphous phase on

quenching depends on the composition of the slag and the equilibration temperature. The most significant problems were observed with high-iron oxide slags in wustite, spinel, and fayalite primary phase fields, where the areas of glassy homogeneous slag phase were limited to locations at the surfaces, directly contacting the quenching medium. The approach used to obtain accurate, repeatable, and objective measurements by EPMA-line analysis was similar to the one described by Nikolic *et al*.,[31] in which the average composition of the liquid phase is calculated from 20 points measured in a well-quenched area within 15 mcm from the surface, with the allowed limit of standard deviation < 1 wt pct. In cases of difficult quenching, the experiments were repeated many times until an area of appropriate well-quenched microstructure was found. However, even with these advanced techniques, it was impossible to obtain accurate results in spinel or wustite phase fields at 1473 K (1200 °C) or higher.

The absence of evaporation loss of Pb species during EPMA measurement of a single point up to 1 minute was confirmed in the present study. The accuracy of the EPMA measurements was estimated to be within 1 wt pct, and the typical detection limit of minor components was estimated to be about 0.01 wt pct.[11] The major uncertainty sources of the results include deviation from targeted temperature and other experimental conditions; phase inhomogeneity due to incomplete achievement of equilibrium and segregation on quenching; sample contamination due to initial reagent impurities; surface roughness; EPMA standard analysis uncertainties; electron beam stability; EPMA ZAF correction inaccuracies (see section II.C below). Special attention was given in this study to test and minimize all potential sources of uncertainties.

B. *Confirmation of Achievement of Equilibrium*

To ensure the achievement of equilibrium in the samples, several measures were used[28,32] including (1) variation of equilibration time; (2) assessment of the compositional homogeneity of phases by EPMA; (3) approaching the final equilibrium point from different starting conditions; and, importantly, (4) consideration of reactions specific to this system that may affect the achievement of equilibrium or reduce the accuracy. Several dedicated series of experiments were carried out for these purposes.

For example, the equilibration of samples in the Pb-Fe-Si-O system in equilibrium with metallic Pb can be approached by starting with the following:

(1) "$FeO_{1.05}$" + PbO + SiO_2 powder mixture, which reacts to form Fe_2O_3-FeO-PbO-SiO_2 slag and liquid Pb metal;
(2) Fe_2O_3 + Pb + SiO_2 or Fe_2O_3 + Pb + PbO + SiO_2 mixtures, where some Pb reacts with Fe_2O_3 to form PbO and FeO, which become components of the liquid slag;
(3) Fe_2O_3 + Fe + Pb + SiO_2 or Fe_2O_3 + Fe + PbO + SiO_2 mixtures, where Fe reacts with Fe_2O_3 to form FeO as a slag component, and may also reduce PbO to Pb; and
(4) mixtures of lead silicate (PbO-SiO_2) and/or fayalite (FeO-SiO_2) master-slags, with the addition of SiO_2, Fe_2O_3, "$FeO_{1.05,}$" PbO, and metallic Pb.

All these options were explored in dedicated series of experiments. It was found that:

(a) Simultaneous presence of two high melting temperature oxides (particularly Fe_2O_3 and SiO_2) usually results in slow dissolution of both in the slag. After fast transformation of Fe_2O_3 into Fe_3O_4 (which is still high-melting), the non-equilibrium phase combination of slag + tridymite + spinel can exist for many hours. Only with the help of significant premelt (up to 1573 K (1300°C)), it can be transformed to the equilibrium phase assemblage, such as, slag + tridymite, and slag + tridymite + fayalite.

However, this high-temperature premelt has its own disadvantages due to the loss of Pb and PbO from the sample, especially if an open substrate is used. Therefore, fayalite master-slag was first prepared from a mixture of Fe + Fe_2O_3 + SiO_2; this has a melting temperature of <1473 K (1200 °C), compared to ~1868 K (1595 °C) for Fe_3O_4 and 1996 K (1723 °C) for SiO_2.[25] Lead silicate master-slag [the eutectic at 40 mol pct PbO melting < 1013 K (740 °C)] was also used to reduce Pb/PbO vaporization during the initial heating stage, to suppress foaming of the slag, and to enhance homogeneity of the sample.

(b) The reaction of metallic Pb with Fe_2O_3 is kinetically slow (the equilibrium is not achieved within 1 day of heating) due to the limited interfacial area of Pb drops since the metal droplets are not wetting on the oxide surfaces and tend to coalesce. The opposite reaction, where Pb metal is gradually formed by reduction from the slag with excess ferrous iron, was found to be much faster.

(c) Fe_3O_4 crystals formed from Fe_2O_3 in the initial mixture retain very small grain size for extended time of equilibration with the slags at low temperatures [1173 K (900 °C) and below]. This often makes the EPMA measurement of compositions of both those spinel crystals and the slag between them challenging. Again, a significant initial preheating could help but could also result in evaporation of Pb and PbO.

As a conclusion from (b) and (c), the use of Fe_2O_3 or Fe_3O_4 as components of the initial mixtures was avoided; "$FeO_{1.05}$" and the fayalite master-slag FeO-SiO_2, x(SiO_2)~35-40 mol pct were principally used to introduce iron oxides into the system.

III. RESOLVING UNCERTAINTIES OF EPMA ZAF CORRECTION

It was found in the previous studies of PbO-containing slags[1] that the Duncumb-Philibert ZAF correction supplied with JEOL 8200 EPMA[33–35] in the PbO-SiO_2 system has a systematic uncertainty. An additional correction to improve the accuracy of phase

Table I. Composition Ranges of Solid Primary Phases at the PbO-"FeO_x"-SiO_2 Liquidus in Equilibrium with Metallic Pb

Phase Name	Formula	Abbrev.	Current FactSage	Present Study	No. of Points	Composition Range
Cristobalite	SiO_2		yes	yes	1 + 3[†]	< 0.2 pct "FeO", < 0.03 pct PbO*
Tridymite	SiO_2		yes	yes	30 + 8[†]	< 0.75 pct "FeO", < 0.03 pct PbO*
Quartz	SiO_2		yes	yes	6 + 2[†]	< 0.3 pct "FeO", < 0.02 pct PbO*
Spinel	Fe_3O_4		yes	yes	39 + 7[‡]	< 1 pct SiO_2, < 0.09 pct PbO
Wustite	FeO_{1+x}		yes	yes	1	< 0.7 pct SiO_2, < 0.02 pct PbO*
Fayalite	$2FeO{\cdot}SiO_2$	F_2S	yes	yes	15	33.1 to 33.5 pct SiO_2, < 0.03 pct PbO*
Melanotekite	$PbO{\cdot}FeO_{1.5}{\cdot}SiO_2$	PFS	yes	yes	6	32.5 to 33.3 pct SiO_2, 32.9 to 33.4 pct PbO
Barysilite	$8PbO{\cdot}FeO{\cdot}6SiO_2$	P_8FS_6	no	yes	14 + 1[§]	39.0 to 40.3 pct SiO_2, 52.9 to 54.1 pct PbO
Melilite	$2PbO{\cdot}Fe_2O_3{\cdot}SiO_2$ $2PbO{\cdot}FeO{\cdot}2SiO_2$		yes	no	—	**
5-lead iron silicate	$5PbO{\cdot}FeO_{1.5}{\cdot}SiO_2$	P_5FS	yes	yes	5 + 2[§]	12.7 to 14.5 pct SiO_2, 71.4 to 72.2 pct PbO
6-lead iron silicate	$6PbO{\cdot}FeO_{1.5}{\cdot}SiO_2$ $6PbO{\cdot}(1+x)FeO_{1.5}{\cdot}(1-x)SiO_2$	P_6FS $P_6F_{1+x}S_{1-x}$	no	yes	5 + 3[§]	9.0 to 12.7 pct SiO_2, 73.3 to 75.3 pct PbO
Magnetoplumbite	$(1+x)PbO{\cdot}xFeO{\cdot}(12-2x)FeO_{1.5}$, $0 < x < 1$	$P_{1+x}F_{12-x}$	$PbFe_{10}O_{16}$	yes	3 + 2[§]	Fe:Pb = 5.5 to 12
Plumboferrite	$PbO{\cdot}(5+x)FeO_{1.5}$, $0 < x < 1$	PF_{5+x}	$PbFe_4O_7$	no[¶]	—	Fe:Pb = 5 to 6
1:1 lead ferrite	$PbO{\cdot}(1 \pm x)FeO_{1.5}$, $0 < x < 0.2$	$PF_{1\pm x}$	$Pb_2Fe_2O_5$	no	0 + 3[‡]	Fe:Pb = 0.9 to 1.1
Alamosite	$PbO{\cdot}SiO_2$	PS	yes	yes	1[§] + 6[†]	**
Lead orthosilicate	$2PbO{\cdot}SiO_2$	P_2S	yes	yes	6 + 3[§]	32.4 to 33.8 pct SiO_2, 0 to 1.7 pct "FeO"
11:3 lead silicate	$11PbO{\cdot}3SiO_2$ $11PbO{\cdot}xFeO_z{\cdot}(3-x)SiO_2$	$P_{11}S_3$ $P_{11}F_xS_{3-x}$	Pb_4SiO_6	yes	2 + 1[§]	19.5 to 21.5 pct SiO_2, 0 to 1.8 pct "FeO"
5-lead silicate	$5PbO{\cdot}SiO_2$	P_5S	no	no[$]	—	**
Massicot	PbO		yes	yes	9 + 3[§]	< 0.05 pct SiO_2*, < 0.12 pct "FeO"

All concentrations are in mol pct.
*Below detection limit.
**No data available.
[†]Also observed in the study of the PbO-SiO_2 system (in air and in equilibrium with metallic Pb).
[‡]Also observed in the study of the Pb-Fe-O system in equilibrium with metallic Pb.
[§]Including subsolidus equilibria.
[¶]Observed in the study of the Pb-Fe-O system,[41] but only in air.
[$]Observed in the study of the PbO-SiO_2 system only at subsolidus conditions.

Table II. Experimental Compositions of Phases in the PbO-"FeO"-SiO_2 System in Equilibrium with Metallic Pb

Exp. No.	Substrate	Premelt/ Precrystallization T [K (°C)]	Final Equilibration *T* [K (°C)]	Time, h*	Phase	Composition (Mol Pct) PbO	FeO	SiO_2
SiO_2 (quartz and tridymite) liquidus								
1	SiO_2 amp.	1193 (920)	983 (710)	2 + 68	Liquid	35.0	9.7	55.3
					Quartz	n.a.		~ 100
2	SiO_2 amp.	1373 (1100)	1073 (800)	10 + 48	Liquid	34.1	9.9	56.1
					Quartz	n.a.		~ 100
3	SiO_2 amp.	1373 (1100)	1273 (1000)	1 + 20	Liquid	30.8	11.1	58.1
					Tridymite	*0.00*	*0.08*	99.92
4	SiO_2 amp.	1473 (1200)	1373 (1100)	3 + 20	Liquid	28.9	10.6	60.4
					Tridymite	*0.01*	*0.06*	99.93
5	SiO_2 amp.	1473 (1200)	1373 (1100)	4 + 17	Liquid	23.5	21.5	55.0
					Tridymite	*0.02*	0.11	99.88
6	SiO_2 amp.	1503 (1230)	1373 (1100)	1 + 17	Liquid	16.8	34.5	48.6
					Tridymite	*0.01*	0.27	99.72
7	SiO_2 c.c.	1603 (1330)	1423 (1150)	2 + 3	Liquid	5.6	51.3	43.1
					Tridymite	*0.00*	*0.00*	99.41
8	SiO_2 amp.	1573 (1300)	1423 (1150)	1 + 17	Liquid	3.5	54.3	42.3
					Tridymite	*0.00*	0.68	99.32
9	SiO_2 c.c.	1473 (1200)	1423 (1150)	1 + 3	Liquid	18.8	29.3	51.8
					Tridymite	*0.02*	0.22	99.76
10	SiO_2 c.c.	1523 (1250)	1423 (1150)	1 + 3	Liquid	25.2	18.3	56.5
					Tridymite	*0.02*	0.10	99.88
11	SiO_2 amp.	1523 (1250)	1473 (1200)	2 + 17	Liquid	28.5	8.4	63.1
					Tridymite	*0.03*	*0.05*	99.91
12	SiO_2 amp.	1523 (1250)	1473 (1200)	1 + 17	Liquid	16.4	32.1	51.6
					Tridymite	*0.01*	0.22	99.77
13	SiO_2 amp.	1573 (1300)	1473 (1200)	4 + 15	Liquid	12.4	39.5	48.1
					Tridymite	*0.01*	0.32	99.68
14	SiO_2 c.c.	1603 (1330)	1573 (1300)	1 + 3	Liquid	21.4	18.2	60.5
					Tridymite	*0.00*	0.10	99.90
15	SiO_2 c.c.	—	1573 (1300)	3	Liquid	19.8	21.6	58.7
					Tridymite	n.a.		~100
16	SiO_2 amp.	1623 (1350)	1573 (1300)	1 + 3	Liquid	11.8	37.5	50.7
					Tridymite	*0.01*	0.33	99.66
17	SiO_2 amp.	1603 (1330)	1573 (1300)	1 + 4	Liquid	3.3	52.4	44.3
					Tridymite	*0.02*	0.71	99.27
18	SiO_2 c.c.	1693 (1420)	1673 (1400)	0.5	Liquid	21.8	13.1	65.1
					Tridymite	*0.02*	*0.08*	99.90
19	SiO_2 c.c.	1693 (1420)	1673 (1400)	0.5	Liquid	16.0	24.9	59.1
					Tridymite	*0.02*	0.20	99.77
20	SiO_2 amp.	1703 (1430)	1673 (1400)	1 + 3	Liquid	11.9	34.0	54.1
					Tridymite	*0.01*	0.30	99.70
21	SiO_2 amp.	1703 (1430)	1673 (1400)	1 + 4	Liquid	3.7	48.5	47.8
					Tridymite	*0.00*	0.55	99.45
SiO_2 (cristobalite) liquidus								
22	SiO_2 amp.	1883 (1510)	1773 (1500)	2	Liquid	13.1	22.1	64.8
					Cristobalite	*0.01*	0.19	99.80
Tridymite + Fayalite boundary								
23	SiO_2 amp.	1523 (1250)	1273 (1000)	19 + 48	Liquid	18.8	32.7	48.5
					Tridymite	*0.02*	0.22	99.76
					Fayalite	*0.00*	66.8	33.2
24	Fe_3O_4 o.	1393 (1120)	1273 (1000)	0.5 + 20	Liquid	20.1	31.4	48.5
					Tridymite	*0.00*	0.43	99.57
					Fayalite	*0.00*	66.5	33.5
25	SiO_2 o.	1473 (1200)	1323 (1050)	0.5 + 15	Liquid	14.3	39.3	46.4
					Tridymite	*0.01*	0.36	99.63
					Fayalite	*0.01*	66.2	33.7
26	Fe_3O_4 o.	1393 (1120)	1343 (1070)	0.5 + 6	Liquid	12.2	43.1	44.8
					Tridymite	*0.02*	0.49	99.49
					Fayalite	*0.03*	66.6	33.4

Table II. Continued

Exp. No.	Substrate	Premelt/ Precrystallization T [K (°C)]	Final Equilibration *T* [K (°C)]	Time, h*	Phase	Composition (Mol Pct) PbO	FeO	SiO_2
27	SiO_2 o.	1493 (1220)	1343 (1070)	2.5 + 15	Liquid	13.0	41.7	45.3
					Tridymite	*0.02*	0.36	99.62
					Fayalite	*0.03*	66.7	33.2
28	SiO_2 amp.	1463 (1190)	1373 (1100)	1.5 + 17	Liquid	10.6	44.2	45.2
					Tridymite	*0.00*	0.35	99.65
					Fayalite	*0.01*	66.5	33.5
29	SiO_2 o.	1523 (1250)	1393 (1120)	0.5 + 4	Liquid	6.7	51.0	42.3
					Tridymite	*0.01*	0.49	99.50
					Fayalite	*0.01*	66.9	33.1
Tridymite + Fe metal boundary								
30	SiO_2 amp.	1543 (1270)	1488 (1215)	2 + 5	Liquid	0.45	57.2	42.4
					Tridymite	*0.00*	0.69	99.31
					Fe metal	*0.03*	99.97	0.00
					Pb metal	99.38	0.62	0.00
31	SiO_2 amp.	1603 (1330)	1573 (1300)	5	Liquid	0.50	55.2	44.3
					Tridymite	*0.00*	0.74	99.26
					Fe metal	*0.03*	99.97	0.00
					Pb metal	99.20	0.80	0.00
Tridymite or Quartz + Spinel boundary								
32	SiO_2 amp.	1173 (900)	988 (715)	10 + 48	Liquid	35.2	9.6	55.2
					Quartz	*0.03*	*0.09*	99.89
					Spinel	n.a.	~100	
33	SiO_2 o.	1273 (1000)	1023 (750)	4 + 64	Liquid	34.2	10.6	55.2
					Quartz	*0.02*	*0.06*	99.93
					Spinel	n.a.	~100	
34	Fe_3O_4 o.	1223 (950)	1023 (750)	2 + 114	Liquid	35.7	8.1	56.2
					Quartz	*0.00*	0.13	99.87
					Spinel	*0.05*	99.4	0.6
35	FeO_{1+x} c.c.	1223 (950)	1073 (800)	1 + 16	Liquid	31.0	15.1	53.9
					Quartz	n.a.		~100
					Spinel	n.a.	~100	
36	SiO_2 amp.	1273 (1000)	1173 (900)	2 + 20	Liquid	27.5	19.6	52.9
					Tridymite	*0.03*	0.15	99.82
					Spinel	*0.03*	99.52	0.45
37	Fe_3O_4 o.	1403 (1130)	1223 (950)	0.5 + 15	Liquid	24.0	24.9	51.1
					Tridymite	*0.01*	0.16	99.84
					Spinel	*0.07*	99.31	0.62
Fayalite + Spinel boundary								
38	Fe_3O_4 o.	1393 (1120)	1273 (1000)	0.5 + 20	Liquid	20.1	31.4	48.5
					Spinel	*0.04*	99.51	0.45
					Fayalite	*0.00*	66.5	33.5
39	Fe_3O_4 o.	1403 (1130)	1323 (1050)	0.5 + 4	Liquid	16.0	40.1	43.9
					Spinel	*0.02*	99.31	0.67
					Fayalite	*0.00*	66.5	33.5
40	Fe_3O_4 o.	1363 (1090)	1323 (1050)	0.5 + 3	Liquid	15.5	41.6	42.9
					Spinel	n.a.	~100	
					Fayalite	*0.00*	66.7	33.3
41	Fe_3O_4 o.	1393 (1120)	1343 (1070)	0.5 + 6	Liquid	12.2	43.2	44.6
					Spinel	*0.03*	99.22	0.75
					Fayalite	*0.03*	66.6	33.4
42	FeO_{1+x} c.c.	1423 (1150)	1373 (1100)	1.5 + 4	Liquid	11.8	49.5	38.7
					Spinel	*0.04*	99.27	0.70
					Fayalite	*0.03*	66.6	33.3
43	Fe_3O_4 o.	1403 (1130)	1373 (1100)	0.5 + 2	Liquid	11.7	50.4	37.9
					Spinel	n.a.	~100	
					Fayalite	*0.02*	66.8	33.2
44	Fe_3O_4 o.	1443 (1170)	1423 (1150)	1	Liquid	5.0	62.3	32.7
					Spinel	*0.04*	99.11	0.85
					Fayalite	*0.02*	66.8	33.2

Table II. Continued

Exp. No.	Substrate	Premelt/ Precrystallization T [K (°C)]	Final Equilibration *T* [K (°C)]	Time, h*	Phase	Composition (Mol Pct) PbO	FeO	SiO_2
45	Fe_3O_4 o.	1443 (1170)	1423 (1150)	1	Liquid	6.2	61.0	32.8
					Spinel	*0.04*	99.11	0.85
					Fayalite	*0.02*	66.8	33.2
Wustite + Spinel boundary								
46	Fe_3O_4 o.	1473 (1200)	1423 (1150)	0.3 + 1	Liquid	5.2	65.6	29.2
					Spinel	*0.02*	99.33	0.65
					Wustite	*0.02*	99.27	0.71
Fe_3O_4 (spinel) liquidus								
47	Fe_3O_4 o.	1073 (800)	1023 (750)	0.5 + 3	Liquid	70.9	20.6	8.6
					Spinel	n.a.	~100	
48	Fe_3O_4 o.	1223 (950)	1073 (800)	2 + 15	Liquid	52.5	10.9	36.6
					Spinel	n.a.	~100	
49	Ir plate	1173 (900)	1073 (800)	1 + 3	Liquid	69.3	21.8	8.9
					Spinel	n.a.	~100	
50	FeO_{1+x} c.c.	1298 (1025)	1173 (900)	1 + 4	Liquid	38.6	16.8	44.6
					Spinel	*0.07*	99.93	*0.00*
51	FeO_{1+x} c.c.	1298 (1025)	1173 (900)	1 + 4	Liquid	28.5	20.2	51.3
					Spinel	*0.07*	99.93	*0.00*
52	Fe_3O_4 o.	1223 (950)	1173 (900)	1 + 5	Liquid	46.5	15.2	38.3
					Spinel	n.a.	~100	
53	Fe_3O_4 o.	1273 (1000)	1173 (900)	0.5 + 2	Liquid	59.3	18.9	21.8
					Spinel	*0.02*	99.93	*0.05*
54	Fe_3O_4 o.	1273 (1000)	1173 (900)	1 + 2	Liquid	65.7	26.4	7.9
					Spinel	*0.03*	99.97	*0.00*
55	Fe_3O_4 o.	1323 (1050)	1273 (1000)	0.3 + 2	Liquid	30.7	25.3	44.0
					Spinel	n.a.	~100	
56	Fe_3O_4 o.	1373 (1100)	1273 (1000)	0.5 + 3	Liquid	43.3	21.1	35.6
					Spinel	*0.03*	99.90	*0.07*
57	Fe_3O_4 o.	1373 (1100)	1273 (1000)	0.5 + 2	Liquid	54.4	23.1	22.4
					Spinel	*0.08*	99.90	*0.02*
58	Fe_3O_4 o.	1303 (1030)	1273 (1000)	0.5 + 1	Liquid	60.6	32.0	7.5
					Spinel	*0.09*	99.91	*0.01*
59	Fe_3O_4 o.	1373 (1100)	1323 (1050)	0.3 + 1	Liquid	30.4	29.2	40.5
					Spinel	n.a.	~100	
60	Fe_3O_4 o.	no	1323 (1050)	1	Liquid	49.4	25.5	25.1
					Spinel	*0.02*	99.83	0.15
61	Fe_3O_4 o.	no	1323 (1050)	1	Liquid	48.3	25.5	26.2
					Spinel	*0.02*	99.83	0.15
62	Fe_3O_4 o.	no	1373 (1100)	0.3 + 1	Liquid	29.3	33.3	37.4
					Spinel	*0.03*	99.76	0.21
63	Fe_3O_4 o.	1413 (1140)	1373 (1100)	0.5 + 2	Liquid	38.1	29.2	32.7
					Spinel	*0.05*	99.90	*0.05*
64	Fe_3O_4 o.	1393 (1120)	1373 (1100)	0.5 + 1	Liquid	51.8	33.7	14.5
					Spinel	n.a.	~100	
65	Fe_3O_4 o.	1443 (1170)	1423 (1150)	1	Liquid	39.8	33.2	27.0
					Spinel	*0.04*	99.93	*0.04*
66	Fe_3O_4 o.	no	1423 (1150)	1	Liquid	45.6	36.8	17.6
					Spinel	*0.04*	99.94	*0.02*
Spinel + P_8FS_6 (barysilite) boundary								
67	FeO_{1+x} o.	1173 (900)	973 (700)	1 + 3	Liquid	63.9	11.2	24.9
					Spinel	n.a.	~100	
					P_8FS_6	53.4	7.4	39.1
68	Fe_3O_4 o.	1073 (800)	973 (700)	0.5 + 3	Liquid	64.8	10.9	24.3
					Spinel	n.a.	~100	
					P_8FS_6	53.6	7.2	39.2
69	Fe_3O_4 o.	1073 (800)	1023 (750)	0.5 + 3	Liquid	60.9	11.2	27.9
					Spinel	*0.03*	99.94	*0.03*
					P_8FS_6	53.9	7.1	39.0
60	Fe_3O_4 o.	1193/1043 (920/770)	1053 (780)	3 + 15 + 2	Liquid	56.2	11.7	32.1
					Spinel	*0.05*	99.92	*0.03*
					P_8FS_6	53.3	7.2	39.4

Table II. Continued

Exp. No.	Substrate	Premelt/ Precrystallization T [K (°C)]	Final Equilibration *T* [K (°C)]	Time, h*	Phase	Composition (Mol Pct) PbO	FeO	SiO_2
PFS (melanotekite) liquidus								
71	Fe_3O_4 o.	1093 (820)	1053 (780)	2 + 15	Liquid	46.4	8.2	45.4
					PFS	33.2	33.9	32.9
72	Fe_3O_4 o.	1118 (845)	1073 (800)	3 + 9	Liquid	45.9	10.5	43.6
					PFS	32.9	34.0	33.1
PFS (melanotekite) + P_8FS_6 (barysilite) boundary								
73	Ir plate	1123 (850)	981 (708)	12 + 64	Liquid	39.0	4.8	56.2
					P_8FS_6	52.9	7.0	40.1
					PFS	33.0	34.4	32.6
74	Fe_3O_4 o.	1123 (850)	973 (720)	5 + 20	Liquid	39.7	5.2	55.1
					P_8FS_6	53.6	6.9	39.5
					PFS	33.4	34.1	32.5
75	Fe_3O_4 o.	1118 (845)	1023 (750)	5 + 9	Liquid	41.4	6.1	52.6
					P_8FS_6	52.9	6.8	40.3
					PFS	32.9	33.8	33.3
76	Fe_3O_4 o.	1193/1043 (920/770)	1053 (780)	3 + 15 + 2	Liquid	47.1	6.3	46.7
					P_8FS_6	53.3	7.2	39.4
					PFS	33.2	34.3	32.6
P_8FS_6 (barysilite) liquidus								
77	Ir plate	1113/1118 (840/745)	1023 (750)	2 + 3 + 15	Liquid	51.0	1.2	47.8
					P_8FS_6	53.8	6.7	39.5
78	Ir plate	1093/1013 (820/740)	1043 (770)	1 + 16 + 4	Liquid	60.8	4.1	35.2
					P_8FS_6	53.8	6.6	39.6
P_8FS_6 (barysilite) + P_5FS boundary								
79	Fe_3O_4 o.	1123 (850)	943 (670)	10 + 14	Liquid	64.8	11.6	23.7
					P_8FS_6	53.5	7.2	39.3
					P_5FS	71.3	14.1	14.5
P_8FS_6 (barysilite) + P_2S boundary								
80	Ir plate	1073/963 (800/690)	1003 (730)	1 + 60 + 3	Liquid	61.6	4.7	33.7
					P_8FS_6	54.1	6.2	39.7
					P_2S	65.8	0.3	33.9
81	Ir plate	1073/1003 (800/730)	1013 (740)	1 + 16 + 3	Liquid	61.6	1.5	37.0
					P_8FS_6	54.0	6.4	39.6
					P_2S	66.0	0.5	33.6
82	Ir plate	1073/1003 (800/730)	1013 (740)	1 + 16 + 3	Liquid	62.6	3.6	33.8
					P_8FS_6	54.0	6.4	39.6
					P_2S	66.0	0.5	33.6
P_5FS + P_2S boundary								
83	Ir plate	1043/953 (770/680)	963 (690)	2 + 15 + 3	Liquid	67.8	9.1	23.1
					P_5FS	71.7	14.0	14.3
					P_2S	65.9	1.6	32.4
84	Ir plate	1023/958 (750/685)	963 (690)	1 + 15 + 3	Liquid	68.5	8.7	22.8
					P_5FS	71.7	14.2	14.1
					P_2S	65.8	0.9	33.3
P_5FS + $P_{11}S_3$ boundary								
85	Ir plate	1043 (770)	953 (680)	6 + 18	Liquid	68.2	9.6	22.3
					P_5FS	72.2	14.0	13.8
					$P_{11}S_3$	78.6	1.2	20.3
P_5FS + $P_{1+x}F_{12-x}$ (magnetoplumbite) boundary								
86	Fe_3O_4 o.	1043 (770)	963 (690)	1 + 18	Liquid	66.7	11.3	21.9
					P_5FS	72.1	14.2	13.6
					$P_{1+x}F_{12-x}$	17.0	82.4	0.7
87	Ir plate	1103 (830)	973 (700)	4 + 20	Liquid	66.9	13.7	19.4
					P_5FS	72.2	15.1	12.7
					$P_{1+x}F_{12-x}$	15.4	84.6	*0.0*
P_6FS liquidus								
88	Ir plate	1033/953 (760/680)	973 (700)	2 + 3 + 15	Liquid	73.3	7.0	19.7
					P_6FS	75.0	12.2	12.8

Table II. Continued

Exp. No.	Substrate	Premelt/ Precrystallization T [K (°C)]	Final Equilibration T [K (°C)]	Time, h*	Phase	Composition (Mol Pct) PbO	FeO	SiO_2
P_6FS + $P_{11}S_3$ boundary								
89	Ir plate	1023/963 (750/690)	973 (700)	1 + 15 + 3	Liquid	73.8	6.9	19.3
					P_6FS	75.1	12.2	12.7
					$P_{11}S_3$	78.5	1.2	20.4
P_6FS + $P_{1+x}F_{12-x}$ boundary								
90	Ir plate	1123 (850)	1003 (730)	3	Liquid	69.2	15.0	15.8
					P_6FS	74.3	14.7	11.1
					$P_{1+x}F_{12-x}$	16.2	83.8	0.0
P_6FS + PbO (massicot) boundary								
91	Ir plate	1033/973 (760/700)	983 (710)	3 + 15 + 3	Liquid	73.9	8.4	17.6
					P_6FS	75.2	12.9	11.8
					PbO	100.00	*0.00*	*0.00*
92	Ir plate	1033/973 (760/700)	993 (720)	1 + 60 + 3	Liquid	73.7	9.1	17.3
					P_6FS	74.7	12.7	12.6
					PbO	99.86	*0.09*	*0.05*
P_2S liquidus								
93	Ir plate	1043/963 (770/690)	968 (695)	3 + 3 + 17	Liquid	69.5	6.7	23.7
					P_2S	66.0	0.8	33.2
PbO (massicot) liquidus								
94	Ir plate	1043 (770)	988 (715)	2 + 22	Liquid	75.4	5.5	19.1
					PbO	99.88	0.12	*0.00*
95	Ir plate	1043 (770)	988 (715)	1 + 22	Liquid	76.6	2.5	21.0
					PbO	99.88	0.12	*0.00*
96	Ir plate	1033/983 (760/710)	998 (725)	3 + 15 + 3	Liquid	73.7	12.3	14.0
					PbO	99.88	0.12	*0.00*
97	Ir plate	1033 (760)	1013 (740)	18	Liquid	74.4	16.0	9.6
					PbO	99.89	0.11	*0.00*
98	Ir plate	1063 (790)	1023 (750)	1 + 5	Liquid	79.7	2.2	18.1
					PbO	99.92	*0.08*	*0.00*
99	Ir plate	1073 (800)	1023 (750)	1 + 3	Liquid	77.8	4.9	17.4
					PbO	99.95	*0.05*	*0.00*
100	Ir plate	1053 (780)	1023 (750)	6	Liquid	74.3	19.7	6.0
					PbO	99.91	*0.09*	*0.00*
Subsolidus								
101	Fe_3O_4 o.	1103 (840)	943 (670)	2 + 15	P_5FS	71.9	13.8	14.2
					P_2S	65.4	2.2	32.3
					$P_{1+x}F_{12-x}$	20.0	77.9	2.1
102	Ir plate	1073 (800)	953 (680)	1 + 20	P_5FS	71.9	14.1	14.0
					P_2S	66.1	0.8	33.0
103	Ir plate	1023 (750)	963 (690)	1 + 44	P_6FS	75.2	12.1	12.7
					$P_{11}S_3$	78.6	1.3	20.1
					PbO	99.71	0.29	*0.00*
104	Ir plate	1123 (850)	983 (710)	6 + 64	PS	50.8	0.6	48.6
					P_8FS_6	54.0	6.3	39.7
					P_2S	66.3	0.3	33.4
105	Ir plate	1023/963 (750/690)	993 (720)	3 + 15 + 3	P_6FS	75.2	14.9	9.8
					$P_{1+x}F_{12-x}$	17.0	83.0	*0.00*
					PbO	99.89	0.11	*0.00*
106	Ir plate	1033 (760)	1003 (730)	18	P_6FS	73.3	16.7	10.0
					PbO	99.85	0.15	*0.00*

F = FeO or $FeO_{1.5}$ (not Fe_2O_3); cristobalite, tridymite, quartz = SiO_2; spinel (magnetite) = Fe_3O_4; fayalite = F_2S = $2FeO{\cdot}SiO_2$; wustite = FeO_{1+x}; melanotekite = PFS = $PbO{\cdot}FeO_{1.5}{\cdot}SiO_2$; barysilite = P_8FS_6 = $8PbO{\cdot}FeO{\cdot}6SiO_2$; P_5FS = $5PbO{\cdot}FeO_{1.5}{\cdot}SiO_2$; P_6FS = $6PbO{\cdot}FeO_{1.5}{\cdot}SiO_2$; magnetoplumbite = $P_{1+x}F_{12-x}$ = $(1+x)PbO{\cdot}xFeO{\cdot}(12-x)FeO_{1.5}$.

Italic values are those below the estimated detection limit (0.1 mol pct).

Amp: ampoule, o.: open basket or crucible, c.c.: closed cemented crucible, n.a.: not analyzed (due to small crystal size).

*Times are listed as (premelt time) + (equilibration time) or (premelt time) + (precrystallization time) + (equilibration time).

compositions was introduced[36,37] using the following polynomial expression:

$$x_{SiO_2}^{corrected} = x_{SiO_2} - x_{SiO_2}x_{PbO}\left(-0.0129 - 0.0206x_{SiO_2} + 0.421x_{SiO_2}^2 - 0.4066x_{SiO_2}^3\right), \quad [1]$$

where x_{SiO_2} and x_{PbO} are the initial molar fractions of SiO_2 and PbO obtained using the ZAF correction only.

Similarly, it was found that the average observed fayalite ($2FeO{\cdot}SiO_2$) composition is 34.3 mol pct SiO_2, 65.7 mol pct FeO, and negligible (0.02 mol. pct) PbO. However, according to Hillert,[38] the deviation of Si:Fe molar ratio in fayalite from 0.5 is very small (from 0.4984 to 0.5002), so the Si/(Fe + Si) ratio ranges from 33.26 to 33.34 mol pct. No other reference points were available in the "FeO"-SiO_2 binary system at other composition than fayalite (Fe:Si = 2:1). A polynomial that provides maximum correction at $x(SiO_2) = 0.333$ was developed based on the assumption of the systematic overestimate of $x(SiO_2)$, proportional to $x(FeO)$:

$$x_{SiO_2}^{corrected} = x_{SiO_2} - 0.0637x_{FeO}x_{SiO_2}(1 - x_{SiO_2}). \quad [2]$$

Equations [1] and [2] can be applied using the Toop-like extrapolations[39] for samples in the multicomponent systems (*e.g.*, PbO-FeO_x-SiO_2) measured with the same probe at the same EPMA conditions; the correction reduces to 0 when the products $x_{SiO_2}x_{PbO}$ or $x_{SiO_2}x_{FeO}$ respectively approach 0. Only SiO_2 concentrations were adjusted; the ratio of other components is kept the same, due to lack of adequate reference points in the Pb-Fe-O system. The composition correction in the ternary system is expressed as

$$x_{SiO_2}^{corrected} = x_{SiO_2} - x_{SiO_2}x_{PbO}\left(-0.0129 - 0.0206x_{SiO_2} + 0.421x_{SiO_2}^2 - 0.4066x_{SiO_2}^3\right) - 0.0637x_{FeO}x_{SiO_2}(1 - x_{SiO_2}) \quad [3]$$

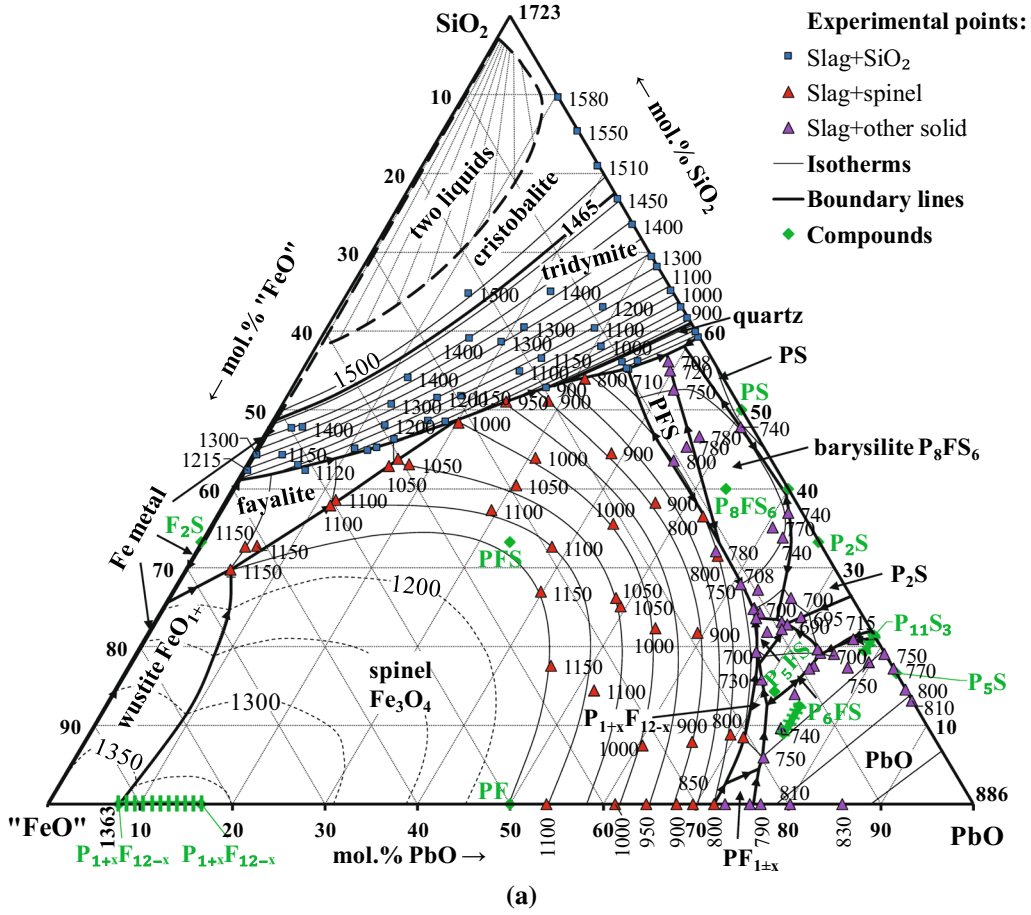

Fig. 2—Liquidus surface of the PbO-"FeO"-SiO_2 system in equilibrium with metallic Pb, including FactSage predictions (for magnetite and wustite primary phase fields at 1473 K (1200 °C) and above) and the isotherms drawn through the experimental points (smoothed polynomial curves). (*a*) complete diagram; (*b*) detail for 40 to 90 mol pct SiO_2 area; (*c*) detail for Pb-rich area. All temperatures are in °C. PbO-SiO_2 and PbO-"FeO" binaries are based on Refs. 37 and 41, respectively. The 1473 K (1200 °C) tridymite isotherm by Hollitt[21] is given for comparison in (b).

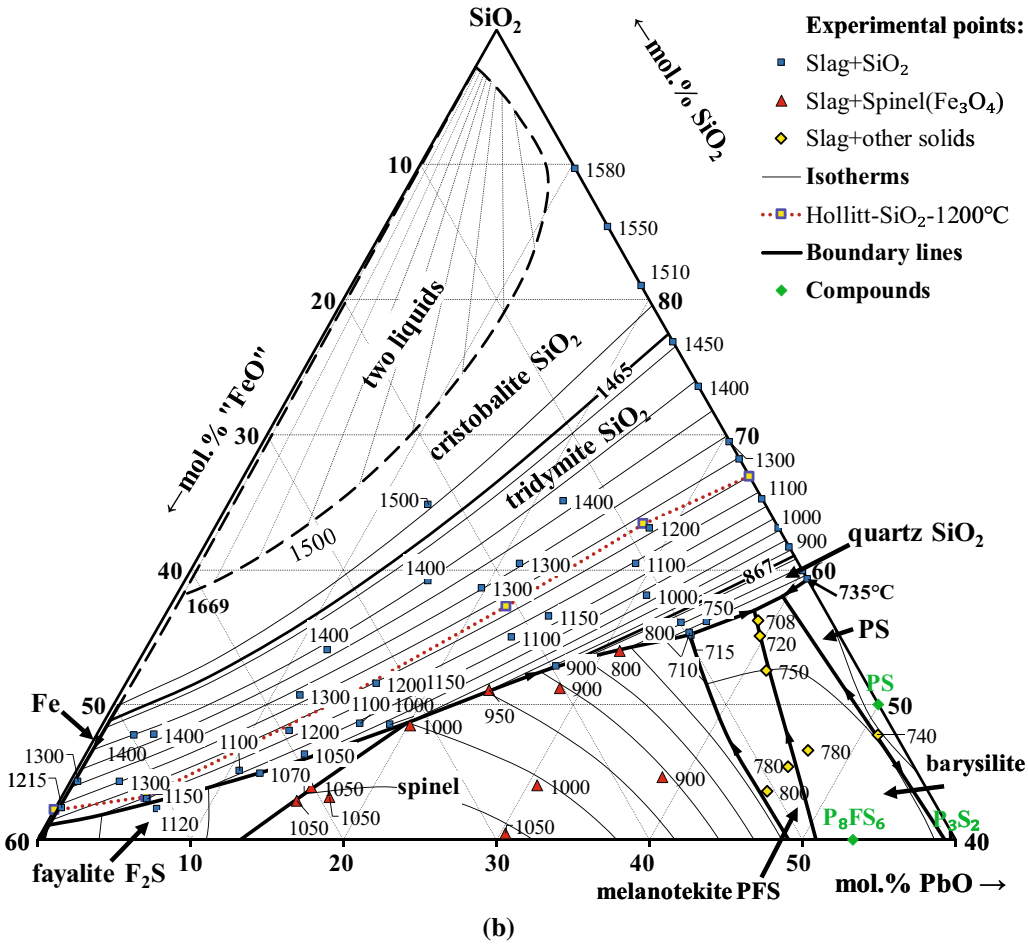

(b)

Fig. 2—continued.

$$x_{\mathrm{PbO}}^{\mathrm{corrected}} = x_{\mathrm{PbO}} \frac{1 - x_{\mathrm{SiO_2}}^{\mathrm{corrected}}}{1 - x_{\mathrm{SiO_2}}}, \quad [4]$$

$$x_{\mathrm{FeO}}^{corrected} = x_{\mathrm{FeO}} \frac{1 - x_{\mathrm{SiO_2}}^{corrected}}{1 - x_{\mathrm{SiO_2}}}. \quad [5]$$

Ternary Pb-Fe-Si-O compounds, such as, melanotekite ($PbO{\cdot}FeO_{1.5}{\cdot}SiO_2$), were not used as reference points for correction, because their possible deviations from stoichiometry were unknown.

IV. RESULTS AND DISCUSSION

Examples of micrographs of quenched PbO-"FeO"-SiO_2 samples are given in Figure 1(a) through (n). All phases observed in the system are listed in Table I. Note that, the abbreviations accepted in the present study are P = PbO, S = SiO_2, F = FeO or $FeO_{1.5}$ (not Fe_2O_3), *i.e.*, the iron atoms are counted regardless of their oxidation state. This facilitates the representation of the EPMA results that do not give accurate information on the oxygen concentration, as well as projecting the concentrations onto the PbO-"FeO"-SiO_2 plane.

Some phases not included into the FactSage database[25] were discovered: barysilite "P_8FS_6" = $8PbO{\cdot}FeO{\cdot}6SiO_2$ and "P_6FS" = $6PbO{\cdot}FeO_{1.5}{\cdot}SiO_2$. On the other hand, other predicted phases (*e.g.*, melilite) were never observed in any sample in the present work, or their compositions were corrected: $Pb_{11}Si_3O_{17}$[37,40] exists instead of Pb_4SiO_6,[25] and $Pb_{1+x}Fe_{12-x}O_{19-x}$ (magnetoplumbite[41]) instead of $PbFe_{10}O_{16}$ and $PbFe_4O_7$.[25] It is known that iron is completely ferrous in fayalite F_2S = $2FeO{\cdot}SiO_2$[38] and barysilite P_8FS_6 = $8PbO{\cdot}FeO{\cdot}6SiO_2$[42] (F = FeO), and ferric in melanotekite PFS = $PbO{\cdot}FeO_{1.5}{\cdot}SiO_2$, 1:1 lead ferrite $PF_{1\pm x}$ = $PbO{\cdot}FeO_{1.5}$, "P_6FS" = $6PbO{\cdot}FeO_{1.5}{\cdot}SiO_2$[22] and supposedly in "$P_5FS$" = $5PbO{\cdot}FeO_{1.5}{\cdot}SiO_2$ (F = $FeO_{1.5}$).[24,25] The oxidation state of Fe changes along the solid solution line of magnetoplumbite $P_{1+x}F_{12-x}$ = $(1 + x)PbO{\cdot}xFeO{\cdot}(12 - 2x)FeO_{1.5}$[41] (the fraction of ferrous iron is within 0 to 10 pct), and was not determined explicitly for $P_6F_{1+x}S_{1-x}$ and $P_{11}F_xS_{3-x}$ solid solutions. Detailed information on the Pb-Si-O and Pb-Fe-O has been presented in the papers.[36,40]

The results of experiments after correction according to Eqs. [1] and [2] are reported in Table II. The phase diagram constructed based on the present results is

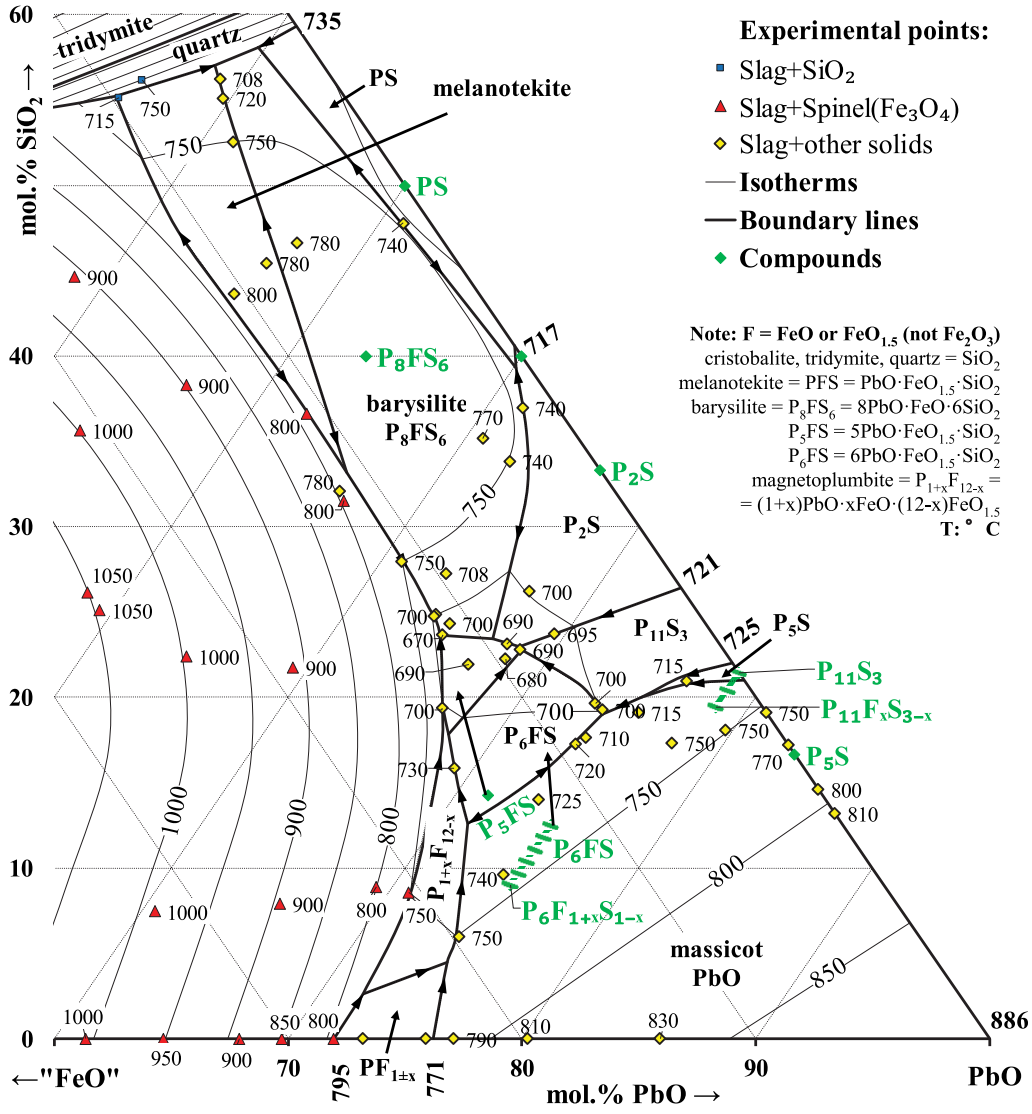

(c)

Fig. 2—continued.

given in Figures 2(a) through (c). The estimated liquidus invariant points involving the observed phases are listed in Table III.

The liquidus in Quartz, Tridymite, and Cristobalite primary phase fields has been determined over a wide range of temperatures, 983 K to 1773 K (710 °C to 1500 °C) and Fe/(Fe + Pb) molar ratios in slag (from 0 at the binary PbO-SiO_2 system[37] to ~ 0.99 at the metallic iron saturation). The slags with PbO contents lower than at the metallic Fe + Pb saturation are not in equilibrium with metallic Pb anymore, because the reaction FeO (slag) + Pb (liq) → Fe (solid) + PbO (slag) would cause metallic Pb to disappear. The Quartz-Tridymite and Tridymite-Cristobalite transitions were not determined directly and accepted from FactSage database[25] as 1144 K and 1742 K (867 °C and 1465 °C), respectively. A wide range of liquid immiscibility is known to exist in the "FeO"-SiO_2 system[43,44] and it is expected to extend over a large part of the ternary PbO-"FeO"-SiO_2 but not reach the binary PbO-SiO_2[37]; it is out of scope of the present study.

The Fayalite (F_2S = Fe_2SiO_4) primary phase field has been determined only along its boundaries with Tridymite and Spinel. The reaction Liquid + Fayalite → Tridymite + Spinel + Pb(liq) is estimated to occur at 1268 K ± 5 K (995 °C ± 5 °C). Only one point was obtained for wustite at 1423 K (1150 °C) in equilibrium with liquid, Pb metal, and spinel; Liquid + Fayalite + Pb equilibrium was observed for a point of a close liquid composition that allows to estimate the reaction Wustite + Liquid → Spinel + Fayalite + Pb(liq) to occur at 1423 K ± 10 K (1150 °C ± 10 °C).

The Melanotekite (PFS = PbO·$FeO_{1.5}$·SiO_2) has been found to form through the peritectic reaction Liquid + Spinel → PFS + Pb(liq) estimated to occur at 1078 K ± 5 K (805 °C ± 5 °C). The Melanotekite primary phase field is limited by three ternary invariant points:

Table III. Invariant Points of the PbO-"FeO_x"-SiO_2 Liquidus in Equilibrium with Metallic Pb

Reaction	Estimated T, [K(°C)]	Liquid Composition (Mol Pct)		
		PbO	"FeO"	SiO_2
Liquid[1] + Fe(liq) → Liquid[2] + Cristobalite + Pb(liq)	1942 (1669) ± 15	0.6	31	58
Liquid + Fe(fcc) + Tridymite → Fayalite + Pb(liq)	1468 (1195) ± 10	0.4	58	41
Liquid + Fe(fcc) → Fayalite + Pb(liq)	1483 (1210) ± 10	0.4	67	33
Liquid + Fe(fcc) + Wustite → Fayalite + Pb(liq)	1463 (1190) ± 10	0.3	75	25
Liquid + Wustite → Spinel + Fayalite + Pb(liq)	1423 (1150) ± 10	5	65	30
Liquid + Fayalite → Tridymite + Spinel + Pb(liq)	1268 (995) ± 5	20	31	49
Liquid + Spinel → PFS + Pb(liq)	1078 (805) ± 5	45	11	44
Liquid + PFS + Pb(liq) → P_8FS_6 + Spinel	1053 (780) ± 10	56	11	33
Liquid + Pb(liq) → P_8FS_6 + PFS	1058 (785) ± 10	52	9	39
Liquid + Pb(liq) → P_8FS_6	1073 (800) ± 15	53	7	40
Liquid + Spinel → PFS + Quartz + Pb(liq)	983 (710) ± 5	35	10	55
Liquid + PFS + Pb(liq) → Quartz + P_8FS_6	973 (700) ± 10	38	5	57
Liquid → Quartz + PS + P_8FS_6 + Pb(liq)	973 (700) ± 10	39	3	58
Liquid + Pb(liq) → PS + P_8FS_6	1023 (750) ± 10	51	2	47
Liquid + Pb(liq) → PS + P_2S + P_8FS_6	983 (710) ± 10	60	1	39
Liquid + Pb(liq) → P_2S + P_8FS_6	1013 (740) ± 10	62	2	36
Liquid + Pb(liq) → Spinel + P_5FS + P_8FS_6	943 (670) ± 5	64	12	24
Liquid + Pb(liq) → P_2S + P_5FS + P_8FS_6	948 (675) ± 10	67	9	24
Liquid + $P_{1+x}F_{12-x}$ + Spinel → P_5FS + Pb(liq)	973 (700) ± 10	66	14	20
Liquid + $P_{1+x}F_{12-x}$ + P_6FS → P_5FS + Pb(liq)	983 (710) ± 10	68	14	18
Liquid + $PF_{1\pm x}$ + Spinel → $P_{1+x}F_{12-x}$ + Pb(liq)	1043 (770) ± 15	72	25	3
Liquid + $PF_{1\pm x}$ → $P_{1+x}F_{12-x}$ + PbO + Pb(liq)	1028 (755) ± 5	74	21	5
Liquid + PbO + Pb(liq) → $P_{1+x}F_{12-x}$ + P_6FS	1008 (735) ± 5	71	16	13
Liquid + PbO → P_6FS + Pb(liq)	998 (725) ± 10	73	12	15
Liquid + PbO + Pb(liq) → $P_{11}S_3$ + P_6FS	973 (700) ± 5	74	7	19
P_5S → $P_{11}S_3$ + PbO	975 (702) ± 5	75	5	20
Liquid + P_6FS → P_5FS + $P_{11}S_3$ + Pb(liq)	963 (690) ± 5	68	9	23
Liquid + $P_{11}S_3$ → P_5FS + P_2S + Pb(liq)	963 (690) ± 5	68	9	23

Liquid + PFS + Pb(liq) → P_8FS_6 + Spinel at 1053 K ± 10 K (780 °C ± 10 °C),

Liquid + Spinel → PFS + Quartz + Pb(liq) at 983 K ± 5 K (710 °C ± 5 °C), and

Liquid + PFS + Pb(liq) → Quartz + P_8FS_6 at 973 K ± 10 K (700 °C ± 10 °C).

It also has a saddle (maximum) point on the boundary line with Barysilite (P_8FS_6):

Liquid + Pb(liq) → P_8FS_6 + PFS at 1058 K ± 10 K (785°C ± 10°C).

The highest of the measured Barysilite liquidus temperatures in points surrounding the Barysilite composition is 1053 K (780 °C); the Barysilite was therefore estimated to melt congruently at 1073 K ± 15 K (800 °C ± 15 °C). In addition to the invariant points on the boundary with Melanotekite described above, Barysilite is also involved into four invariant reactions:

Liquid → Quartz + PS + P_8FS_6 + Pb(liq) at 973 K ± 10 K (700°C ± 10°C),

Liquid + Pb(liq) → PS + P_2S + P_8FS_6 at 983 K ± 10 K (710 °C ± 10 °C),

Liquid + Pb(liq) → Spinel + P_5FS + P_8FS_6 at 943 K ± 5 K (670 °C ± 5 °C), and

Liquid + Pb(liq) → P_2S + P_5FS + P_8FS_6 at 948 K ± 10 K (675 °C ± 10 °C),

as well as two saddle points:

Liquid + Pb(liq) → PS + P_8FS_6 at 1023 K ± 10 K (750°C ± 10°C) and

Liquid + Pb(liq) → P_2S + P_8FS_6 at 1013 K ± 10 K (740 °C ± 10 °C).

The phases P_5FS and P_6FS melt incongruently at 975 K ± 5 K (702 °C ± 5 °C) and 998 K ± 5 K

(725 °C ± 5 °C), respectively. Their primary phase fields are surrounded by the Spinel, Barysilite, P_2S, $P_{11}S_3$, PbO, and Magnetoplumbite primary phase fields, with the following invariant reactions being suggested:

$$\text{Liquid} + \text{Pb(liq)} \rightarrow \text{Spinel} + P_5FS + P_8FS_6 \text{ at } 943\ \text{K} \pm 5\ \text{K}\ (670\ ^\circ\text{C} \pm 5\ ^\circ\text{C})$$

$$\text{Liquid} + \text{Pb(liq)} \rightarrow P_2S + P_5FS + P_8FS_6 \text{ at } 948\ \text{K} \pm 10\ \text{K}\ (675^\circ\text{C} \pm 10^\circ\text{C})$$

$$\text{Liquid} + P_{1+x}F_{12-x} + \text{Spinel} \rightarrow P_5FS + \text{Pb(liq)} \text{ at } 973\ \text{K} \pm 10\ \text{K}\ (700\ ^\circ\text{C} \pm 10\ ^\circ\text{C})$$

$$\text{Liquid} + P_{1+x}F_{12-x} + P_6FS \rightarrow P_5FS + \text{Pb(liq)} \text{ at } 983\ \text{K} \pm 10\ \text{K}\ (710^\circ\text{C} \pm 10^\circ\text{C})$$

$$\text{Liquid} + \text{PbO} + \text{Pb(liq)} \rightarrow P_{1+x}F_{12-x} + P_6FS \text{ at } 1008\ \text{K} \pm 5\ \text{K}\ (735\ ^\circ\text{C} \pm 5\ ^\circ\text{C})$$

$$\text{Liquid} + \text{PbO} + \text{Pb(liq)} \rightarrow P_{11}S_3 + P_6FS \text{ at } 973\ \text{K} \pm 5\ \text{K}\ (700\ ^\circ\text{C} \pm 5\ ^\circ\text{C})$$

$$\text{Liquid} + P_6FS \rightarrow P_5FS + P_{11}S_3 + \text{Pb(liq)} \text{ at } 963\ \text{K} \pm 5\ \text{K}\ (690\ ^\circ\text{C} \pm 5\ ^\circ\text{C})$$

The 1:1 lead ferrite ($PF_{1\pm x}$), Alamosite (PS), and 5-lead silicate (P_5S) were not observed in equilibrium with liquid in any sample in the present study, so their primary phase fields were estimated based on the data for the silica-free Pb-Fe-O system in equilibrium with metallic Pb[41] and iron-free PbO-SiO_2 system in air[37]

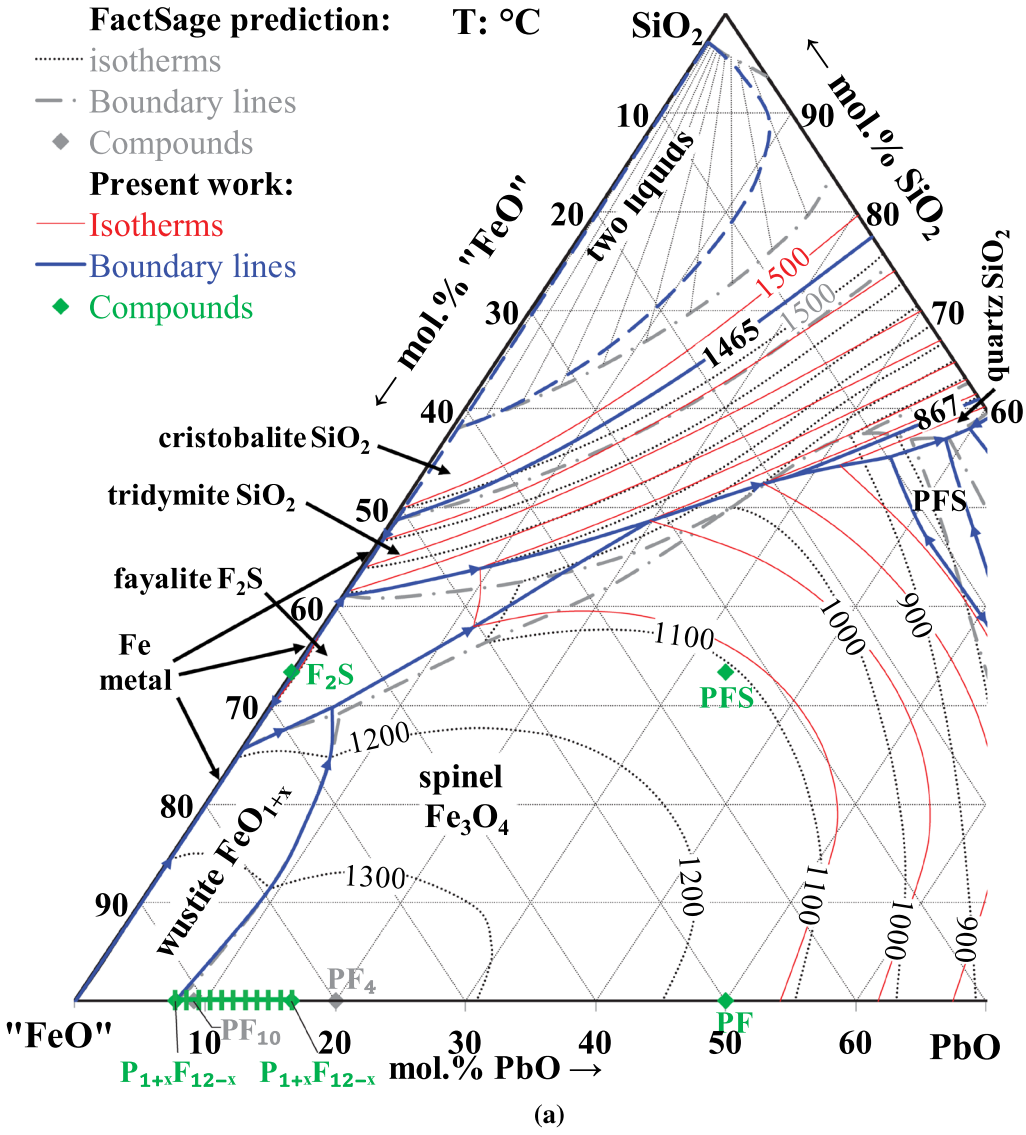

Fig. 3—Comparison of the experimental liquidus surface of the PbO-"FeO"-SiO_2 system in equilibrium with metallic Pb with the initial FactSage prediction. All temperatures are in °C. (*a*) Detail for Tridymite and Spinel primary phase fields; (*b*) detail for PbO-rich range of the diagram.

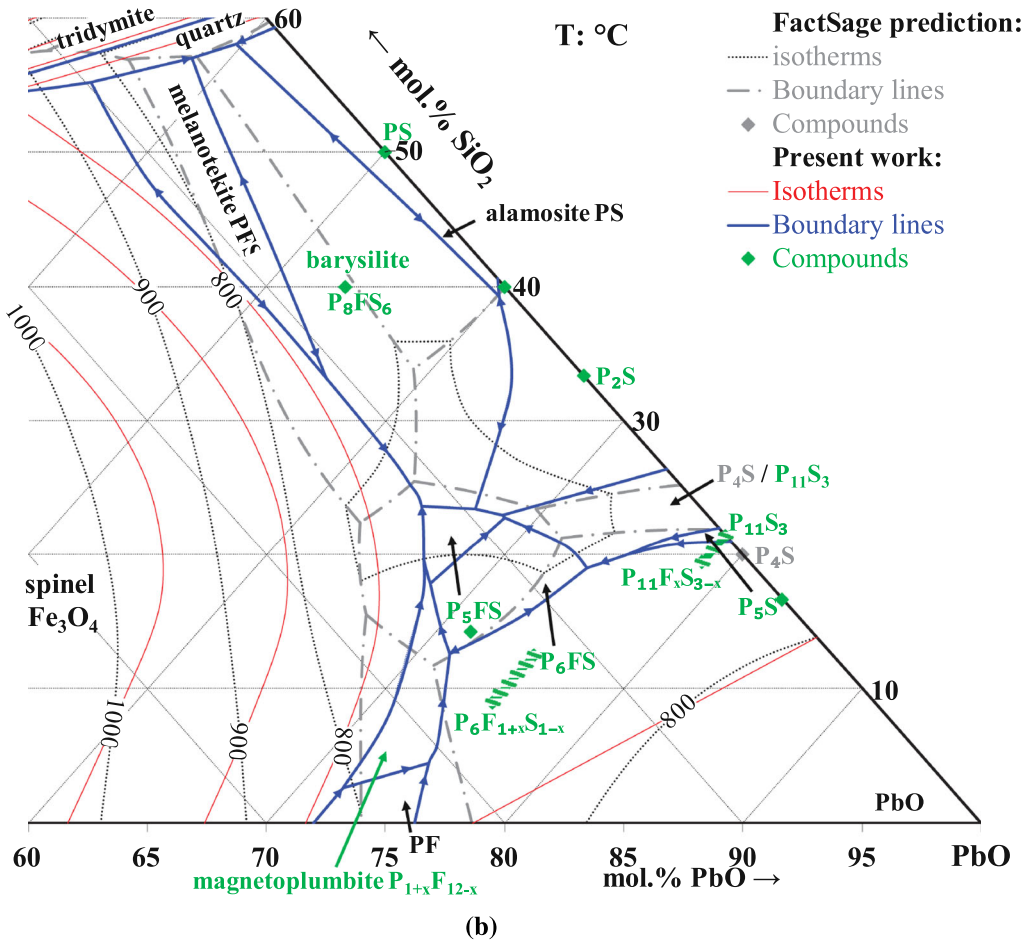

(b)

Fig. 3—continued.

that have been published recently. The reaction $P_5S \rightarrow P_{11}S_3 + PbO$ is estimated to occur at 975 K ± 5 K (702 °C ± 5 °C) assuming that it is not affected by the presence of iron-containing slag and Pb metal. The compound $P_3S_2 = Pb_3Si_2O_7$ ("lead barysilite" or pyrosilicate) is supposed to be stable only at < 955 K (<682 °C), *i.e.*, below the solidus in the Pb-Fe-Si-O system as well as in the binary PbO-SiO_2 system.[37]

The lead ferrite with the Fe:Pb atomic ratio of 5 to 6 was found in several samples; based on the results for the Pb-Fe-O system,[41] it belongs to the Magnetoplumbite solid solution range $P_{1+x}F_{12-x} = Pb_{1+x}Fe_{12-x}O_{19-x}$, $0 < x < 1$, where x tends to have higher values at the reducing conditions (in equilibrium with metal). Plumboferrite (PF_{5+x}) is not expected to be stable in equilibrium with metal.[41] The primary phase fields of Magnetoplumbite ($P_{1+x}F_{12-x}$) and 1:1 lead ferrite ($PF_{1\pm x}$) in the Pb-Fe-Si-O liquidus surface were plotted tentatively only. The primary phase field of $PF_{1\pm x}$ is assumed to be small in size and limited by the invariant reactions

$$\text{Liquid} + PF_{1\pm x} + \text{Spinel} \rightarrow P_{1+x}F_{12-x} + \text{Pb(liq)} \text{ at } 1043 \text{ K} \pm 15 \text{ K } (770 \text{ °C} \pm 15 \text{ °C}), \text{ and}$$

$$\text{Liquid} + PF_{1\pm x} \rightarrow P_{1+x}F_{12-x} + PbO + \text{Pb(liq)} \text{ at } 1028 \text{ K} \pm 5 \text{ K } (755 \text{ °C} \pm 5 \text{ °C}).$$

Other invariant reactions that belong to the systems PbO-SiO_2[37] and Pb-Fe-O in equilibrium with metallic Pb[41] have been described in the corresponding papers.

In the concentration and temperature ranges in which no experiments have been undertaken (particularly for high-iron slags), the isotherms are plotted according to the current FactSage model.[25] The experimental and predicted isotherms and primary phase field boundaries are compared in Figures 3(a) through (b). Most of the observed tridymite and cristobalite liquidus is 50 K to 100 K below the predicted by the current FactSage database. The tridymite and quartz liquidus at low iron concentrations and low temperatures have the opposite tendency; they are 50 K to 100 K higher than predicted. The PbO concentration in the slag along the univariant line Liquid + Tridymite + Fe(fcc) + Pb(liq) at 1473 K to 1573 K (1200 °C to 1300 °C) was found to be higher by a factor of ~2 times than in the results reported by Kudo *et al.*[12] (Figure 4) obtained using wet chemical analysis of the slag. The 1473 K (1200 °C) isotherm is in

a good agreement with the data by Hollitt[21] (Figure 2(b)).

The 1073 K to 1273 K (800 °C to 1000 °C) isotherms in the spinel primary field show the greatest deviations between the experimental and predicted coordinates (Figure 3(a)): it is 4 mol pct "FeO" lower at 20 to 30 mol pct SiO_2 in slag, and 5 mol pct "FeO" higher at 50 to 55 mol pct SiO_2. The fayalite and melanotekite primary phase fields have similar shape and size to those predicted by FactSage.

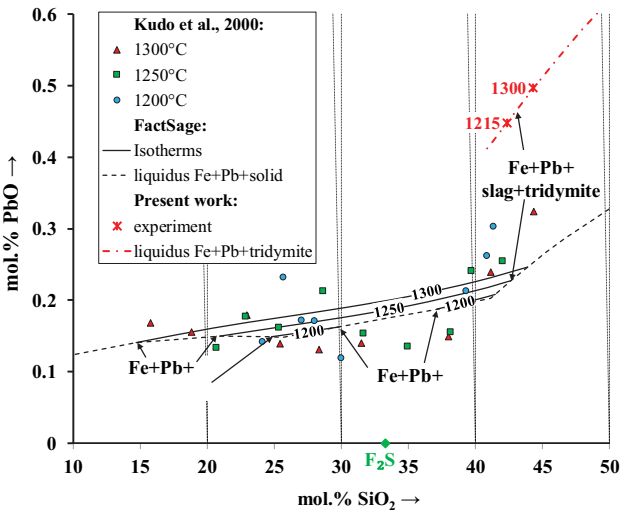

Fig. 4—Detail of the Pb-Fe-Si-O system in equilibrium with both Pb and Fe metals. Two points of the present work (Liquid + Tridymite + Pb + Fe) are compared to the data by Kudo *et al.*[12] and the FactSage model (lines).

A. *Solid Solution Ranges in the PbO-"FeO"-SiO_2 System in Equilibrium with Metallic Pb*

The ranges of compositions of the observed solid oxide phases in the PbO-"FeO"-SiO_2 system in equilibrium with metallic Pb are listed in Table I. Cristobalite, tridymite, and quartz showed limited solubility of iron oxide (Figure 5), which reached 0.75 mol. pct "FeO" for equilibrium with the slags of the highest iron concentration close to the invariant point Liquid + Fe(fcc) + Tridymite = Fayalite + Pb(liq). This is in agreement with the results for the Ca-Fe-Si-O system[45,46] and for the Cu-Fe-Si-O system.[27] None of the silica polymorphs (including the points in the PbO-SiO_2 system[37]) showed any significant solubility of PbO, < 0.03 mol pct, which is below the estimated minimum detection limit.

The solubility of silica and PbO in spinel (Figure 6) is below 1 mol pct SiO_2 and <0.09 mol pct PbO, respectively. This is consistent with the results for the system Pb-Fe-O in equilibrium with metallic Pb[41]; however, significant solubility of PbO in spinel, up to 2 to 3 mol pct, was observed in more oxidizing conditions (Liquid + Spinel + Magnetoplumbite equilibria[41]). The solubility of SiO_2 in spinel is of the same order as found in References 45 and 46 for

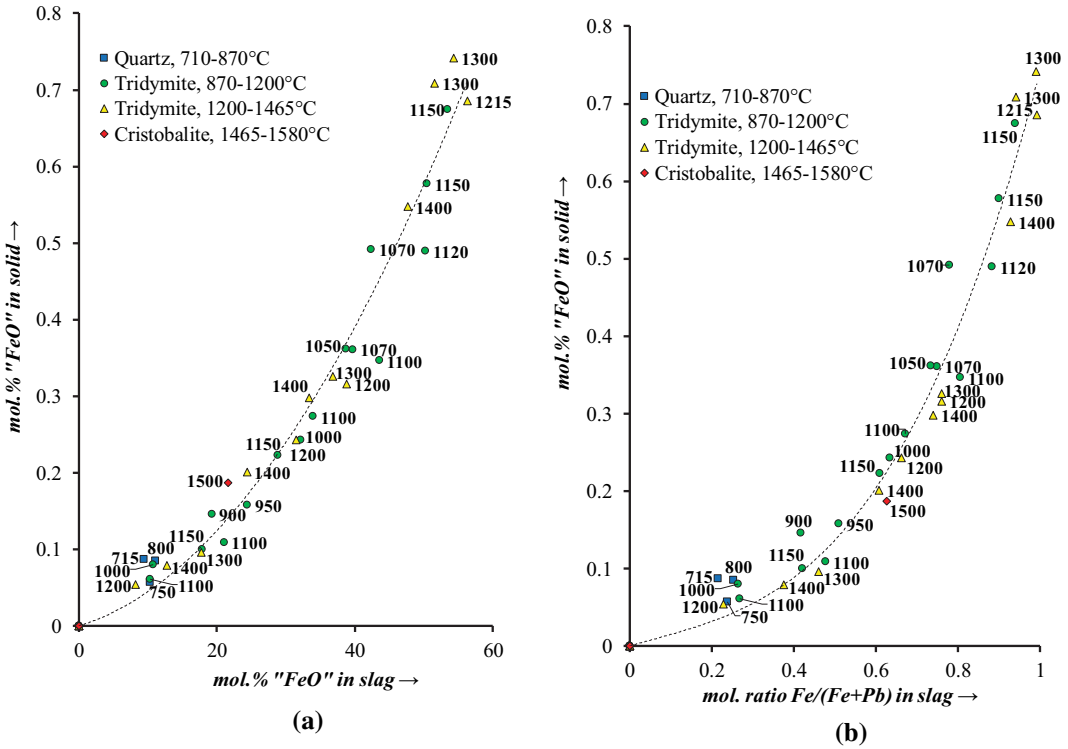

Fig. 5—Iron oxide concentrations in solid quartz, tridymite, and cristobalite crystals in equilibrium with slags of the PbO-"FeO"-SiO_2 system and metallic Pb, as a function of "FeO" concentration (*a*) and molar ratio Fe/(Fe + Pb) (*b*) in the slag. Labels indicate the experimental temperatures (°C).

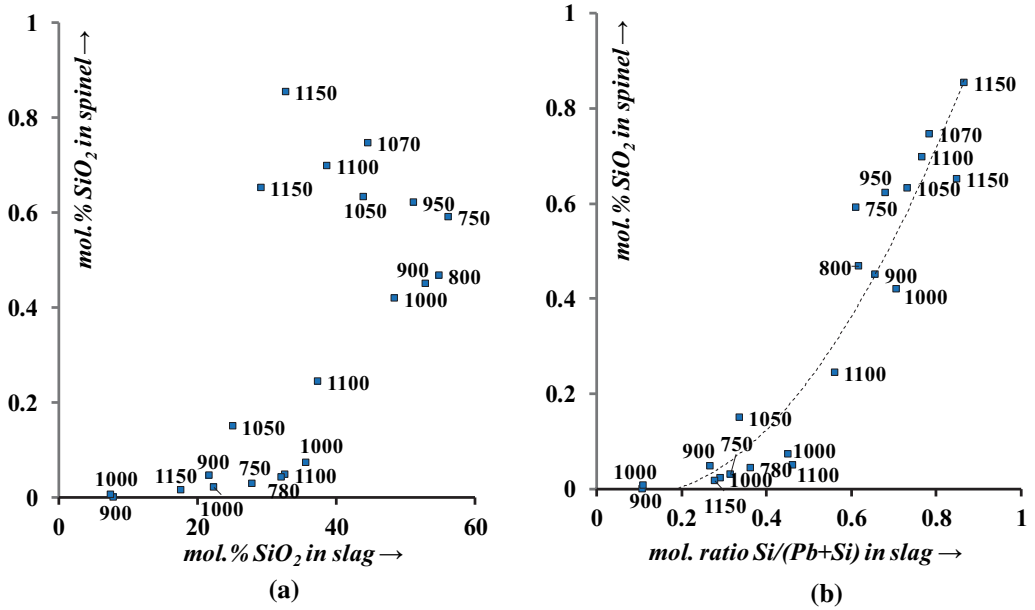

Fig. 6—Silica concentrations in Spinel crystals in equilibrium with slags of the PbO-"FeO"-SiO_2 system and metallic Pb, as a function of SiO_2 concentration (*a*) and molar ratio Si/(Pb + Si) (*b*) in the slag. Labels indicate the experimental temperatures (°C).

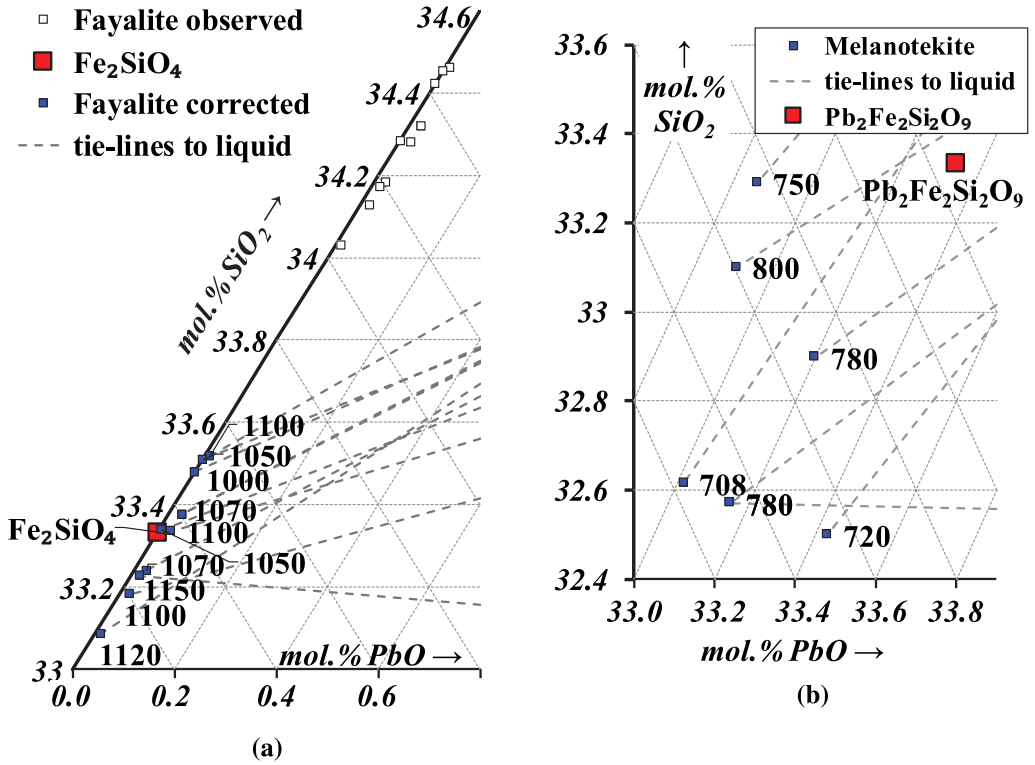

Fig. 7—Fayalite F_2S (*a*) and melanotekite PFS (*b*) compositions measured on crystals in contact with slags of the PbO-"FeO"-SiO_2 system in equilibrium with metallic Pb. Labels indicate the experimental temperatures (°C).

the Ca-Fe-Si-O system and[27] for the Cu-Fe-Si-O system.

The observed solubility of iron oxide in the silica polymorphs cannot be explained by secondary fluorescence in EPMA, because the energy of Kα X-rays emitted by the excited Si atoms is lower than needed to excite the Fe atoms. On the other hand, secondary fluorescence could theoretically account for observed

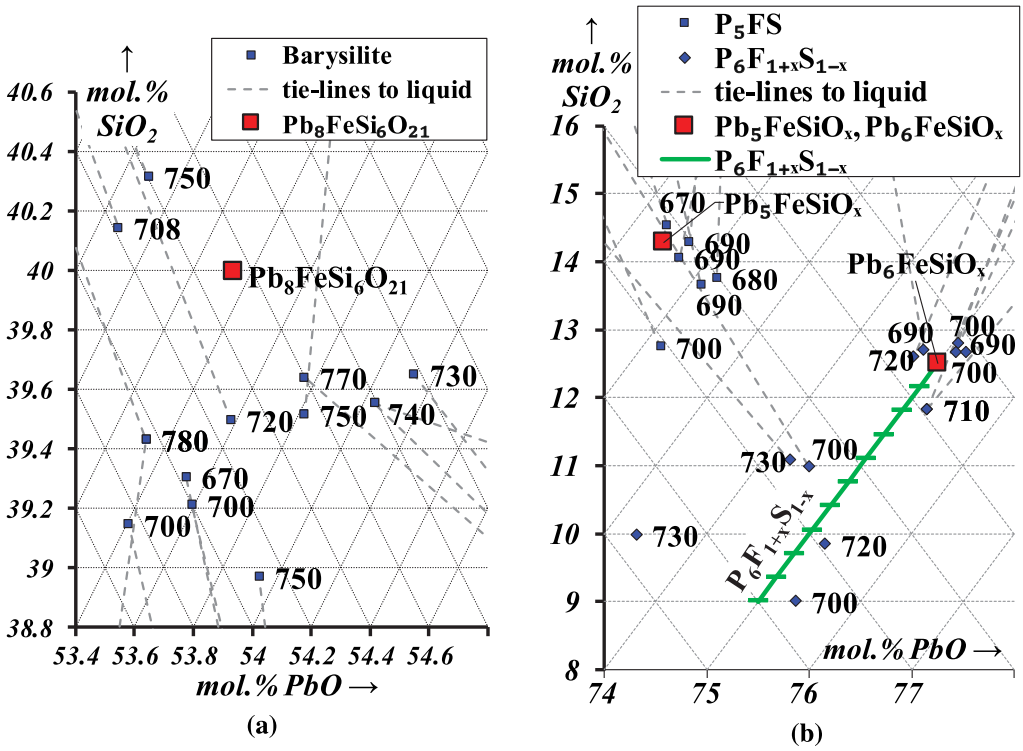

Fig. 8—Barysilite P_8FS_6 (*a*); P_5FS and P_6FS (*b*) compositions measured on crystals in equilibrium with slags (or at subsolidus conditions) of the PbO-"FeO"-SiO_2 system and metallic Pb. Labels indicate the experimental temperatures (°C).

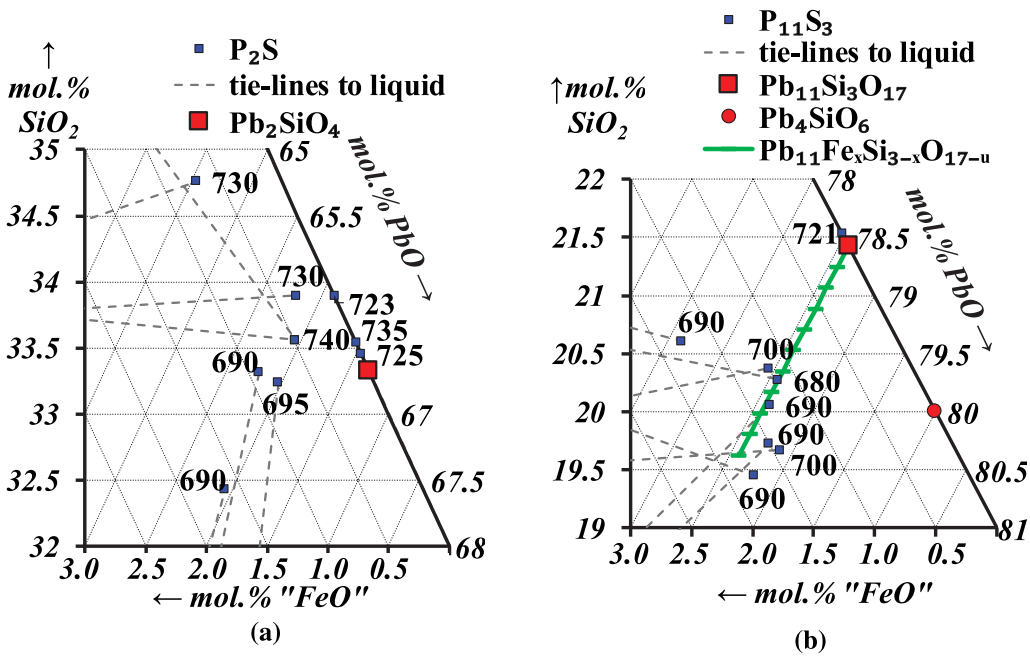

Fig. 9—P_2S (*a*) and $P_{11}S_3$ (*b*) compositions measured on crystals in equilibrium with slags (or at subsolidus conditions) of the PbO-"FeO"-SiO_2 system and metallic Pb. Labels indicate the experimental temperatures (°C).

silica in Spinel. However, in that case, the observed silica concentrations in Spinel would be directly proportional to the silica concentrations in slag, which disagrees with the dependence shown in Figures 6(a) and (b): the solubility of silica in Spinel is higher in equilibrium with the slags (30 to 45 mol pct SiO_2) along the Spinel + Fayalite liquidus boundary line than with the slags highest in silica (55 mol pct SiO_2) along the

Spinel + Quartz boundary line. This confirms that the observed solubilities of silica in Spinel are the actual equilibrium values.

Fayalite was found to have negligible solubility of PbO (Figure 7(a)). Melanotekite (Figure 7(b)) was found to have systematic excess of iron oxide, with the average "FeO_x" concentration of 34.0 mol pct instead of theoretical 33.3 pct. However, this may also be a result of the ZAF correction uncertainty.

Barysilite P_8FS_6 (Figure 8(a)) and P_5FS (Figure 8(b)) were found to have limited ranges of solid solubility, close to the theoretical values. P_6FS (Figure 8(b)) was found to have a range of solutions, which can be approximately described by a formula $P_6F_{1+x}S_{1-x} = 6PbO{\cdot}(1+x)FeO_{1.5}{\cdot}(1-x)SiO_2$, where $0 < x < 0.3$; *i.e.*, part of Si atoms in the P_6FS structure can be substituted with Fe.

Both P_2S and $P_{11}S_3$ showed limited solubility of iron oxide up to 1.7 and 1.8 mol pct, respectively (Figure 9). There is some evidence for preferential substitution of Si atoms with Fe in $P_{11}S_3$, corresponding to the formula $P_{11}F_xS_{3-x} = 11PbO{\cdot}xFeO_{1.5}{\cdot}(3-x)SiO_2$. The shape of the solid solution range for the P_2S phase (Figure 9(a)) has not been determined accurately. The solubilities of silica in magnetoplumbite ($P_{1+x}F_{12-x} = Pb_{1+x}Fe_{12-x}O_{19-x}$) and 1:1 lead ferrite ($PF_{1\pm x} = PbO{\cdot}(1 \pm x)FeO_{1.5}$), and of iron oxide in alamosite ($PS = PbO{\cdot}SiO_2$) and $P_5S = PbO{\cdot}5SiO_2$ were not determined. Finally, no significant solubility of either SiO_2 (< 0.05 mol pct) or "FeO" (< 0.12 mol pct) was detected in PbO (massicot).

In summary, present experimental study has produced the first comprehensive dataset for the Pb-Fe-Si-O system in equilibrium with metallic Pb and Fe that is essential for the lead smelting and recycling industry, and will provide valuable new data that can be used to optimize thermodynamic databases of these systems.

V. CONCLUSIONS

New phase equilibria information in the Pb-Fe-Si-O system in equilibrium with metallic lead has been obtained. The studied range of temperatures covered 923 K to 1773 K (670 °C to 1500 °C), and included the equilibria of slag with one or two crystalline phases: quartz, tridymite, cristobalite (SiO_2), spinel (Fe_3O_4), fayalite (Fe_2SiO_4), melanotekite ($PbO{\cdot}FeO_{1.5}{\cdot}SiO_2$), barysilite ($8PbO{\cdot}FeO{\cdot}6SiO_2$), "$P_5FS$" ($5PbO{\cdot}FeO_{1.5}{\cdot}SiO_2$) and "$P_6FS$" ($6PbO{\cdot}FeO_{1.5}{\cdot}SiO_2$) ternary compounds, lead silicates (Pb_2SiO_4, $Pb_{11}Si_3O_{17}$), lead ferrites (magnetoplumbite $Pb_{1+x}Fe_{12-x}O_{19-x}$ solid solution range), and lead oxide (PbO, massicot). Limited (<1 mol pct) ranges of solid solutions of "FeO" in tridymite and SiO_2 in spinel have been detected; "P_6FS" and "$P_{11}S_3$" form 3 and 2 mol pct ranges of solutions where Si atoms are substituted with Fe, corresponding to the formulas $P_6F_{1+x}S_{1-x}$. and $P_{11}F_xS_{3-x}$, respectively. This is the first systematic study of the Pb-Fe-Si-O system in equilibrium with metallic Pb, as a part of the multi-component system Pb-Zn-Fe-Cu-Si-Ca-Al-Mg-O, essential for the lead smelting and recycling industries.

ACKNOWLEDGMENTS

The authors would like to thank Nyrstar (Australia), Outotec Pty Ltd (Australia), Aurubis AG (Germany), Umicore NV (Belgium), and Kazzinc Ltd, Glencore (Kazakhstan), and Australian Research Council Linkage Project LP150100783 for their financial support for this research. The authors are grateful to Prof. P.C. Hayes (UQ) for valuable comments and suggestions.

REFERENCES

1. E. Jak: Phase Equilibria to Characterise Lead/Zinc Smelting Slags and Sinters (PbO-ZnO-CaO-SiO_2-Fe_2O_3-FeO). Ph.D Thesis, University of Queensland, 1995.
2. E. Jak, S.A. Decterov, P. Wu, P.C. Hayes, and A.D. Pelton: *Metall. Mater. Trans. B*, 1997, vol. 28B, pp. 1011–18.
3. E. Jak, S.A. Decterov, P.C. Hayes, and A.D. Pelton: *Can. Metall. Q.*, 1998, vol. 37, pp. 41–47.
4. E. Jak, N. Liu, and P.C. Hayes: *Metall. Mater. Trans. B*, 1998, vol. 29B, pp. 541–53.
5. E. Jak, B. Zhao, P.C. Hayes, S.A. Decterov, and A.D. Pelton: in *Zinc and Lead Processing*, J.E. Dutrizac, J.A. Gonzalez, G.L. Bolton, and P. Hancock, eds., Met. Soc. CIMM, 1998, pp. 313–33.
6. E. Jak, B. Zhao, N. Liu, and P.C. Hayes: *Metall. Mater. Trans. B*, 1999, vol. 30B, pp. 21–27.
7. E. Jak and P.C. Hayes: *Metall. Mater. Trans. B*, 2002, vol. 33B, pp. 817–25.
8. E. Jak and P.C. Hayes: *Metall. Mater. Trans. B*, 2002, vol. 33B, pp. 851–63.
9. E. Jak and P.C. Hayes: *Metall. Mater. Trans. B*, 2003, vol. 34B, pp. 369–82.
10. E. Jak, B. Zhao, I. Harvey, and P.C. Hayes: *Metall. Mater. Trans. B*, 2003, vol. 34B, pp. 383–97.
11. E. Jak, P.C. Hayes, and H.-G. Lee: *Met. Mater. (Seoul)*, 1995, vol. 1, pp. 1–8.
12. M. Kudo, E. Jak, P.C. Hayes, K. Yamaguchi, and Y. Takeda: *Metall. Mater. Trans. B*, 2000, vol. 31B, pp. 15–24.
13. M.E. Schlesinger and C.C. Lynch: *Metall. Trans. B*, 1986, vol. 17B, pp. 817–27.
14. N. Moon, M. Hino, Y. Lee, and K. Itagaki: *Proc. Int. Conf. Molten Slags, Fluxes Salts '97, 5th*, 1997, pp. 753–59.
15. N. Moon, M. Hino, Y. Lee, and K. Itagaki: *Shigen to Sozai*, 1998, vol. 114, pp. 121–26.
16. N. Moon, M. Hino, Y. Lee, and K. Itagaki: *Metall. Rev. MMIJ*, 1998, vol. 15, pp. 38–62.
17. N. Moon, M. Hino, Y. Lee, and K. Itagaki: *Metall. Rev. MMIJ*, 1999, vol. 16, pp. 179–93.
18. G.B. Hoang and D.R. Swinbourne, *Trans. Inst. Min. Metall. Sect. C*, 2007, vol. 116, pp. 133–38.
19. D. Matsura, S. Ueda, and K. Yamaguchi: *High Temperature Materials and Processes* (Berlin, Germany), 2011, vol. 30, pp. 441–46.
20. J.-L. Wang, X.-C. Wen, and C.-F. Zhang: *Trans. Nonferrous Met. Soc. China*, 2015, vol. 25, pp. 1633–39.
21. M.J. Hollitt, G.M. Willis, and J.M. Floyd, *2nd Intl. Symp. on Metallurgical Slags and Fluxes*, 1984, pp. 497–516.
22. F.P. Glasser: *Am. Mineral.*, 1967, vol. 52, pp. 1085–93.
23. A. Nitta, T. Miura, T. Komatsu, and K. Matusita: *J. Am. Ceram. Soc.*, 1989, vol. 72, pp. 163–65.
24. P. Chartrand, B. Zhao and E. Jak, Phase equilibria of the PbO-"Fe_2O_3"-SiO_2 system in air, Private communication, 1996.
25. E. Jak, S.A. Decterov, P.C. Hayes, and A.D. Pelton: in *Proc. 5th Int. Conf. on Molten Slags, Fluxes and Salts*, Iron and Steel Soc., AIME, Sydney, Australia, 1997, pp. 621–28.
26. *FactSage computer package, Version 6.2 (2010), Databases FToxid and FTmisc.* (Ecole Polytechnique, Montréal, http://www.factsage.com/, 2008).
27. T. Hidayat, H.M. Henao, P.C. Hayes, and E. Jak: *Metall. Mater. Trans. B*, 2012, vol. 43, pp. 1034–45.
28. E. Jak: in *9th Intl. Conf. on Molten Slags, Fluxes and Salts* (MOLTEN12), The Chinese Society for Metals: Beijing, China, 2012.
29. F.D. Richardson: *Platin. Met. Rev.*, 1958, vol. 2, pp. 83–85.

30. B.J. Kennedy: *J. Solid State Chem.*, 1996, vol. 123, pp. 14–20.
31. S. Nikolic, P.C. Hayes, and E. Jak: *Metall. Mater. Trans. B*, 2009, vol. 40B, pp. 892–99.
32. M. Shevchenko, T. Hidayat, P. Hayes, and E. Jak: in *Molten 2016, 10th Intl. Conf. on Molten Slags, Fluxes and Salts*, Seattle, Washington, USA, 2016, pp. 1221–28.
33. J. Philibert, *X-Ray Opt. X-Ray Microanal., 3rd Intl. Symp., Stanford Univ.,* 1963, pp. 379–92.
34. P. Duncumb and S.J.B. Reed: Tube Investments Res. Lab., Cambridge, UK, 1968.
35. P. Duncumb: *Electron Microsc. Anal., Proc. Anniv. Meet., 25th,* 1971, pp. 132–27.
36. M. Shevchenko, J. Chen, and E. Jak: in *AMAS 2017*, *14th Biennial Australian Microbeam Analysis Symposium*, QUT, Brisbane, 2017, pp. 94–95.
37. M. Shevchenko and E. Jak: *J. Am. Ceram. Soc.*, 2017. https://doi.org/10.1007/s11663-017-1136-0.
38. M. Hillert, M. Selleby, and B. Sundman: *Phys. Chem. Miner.*, 1996, vol. 23, pp. 387–90.
39. G.W. Toop and C.S. Samis: *TMS-AIME*, 1962, vol. 224, pp. 878–87.
40. K. Hirota and Y.T. Hasegawa: *Bull. Chem. Soc. Jpn.*, 1981, vol. 54, pp. 754–56.
41. M. Shevchenko and E. Jak: *Metall. Mater. Trans. B,* 2017. https://doi.org/10.1007/s11663-017-1069-7.
42. J. Ito and C. Frondel: *TheAm. Mineral.*, 1967, vol. 52, pp. 1077–84.
43. J.W. Greig: *Am. J. Sci., 5th Ser.*, 1927, vol. 13, pp. 133–54.
44. T. Hidayat, D. Shishin, S.A. Decterov, and E. Jak: *J. Phase Equilib. Diff.*, 2016, pp. 1–16.
45. T. Hidayat, P.C. Hayes, and E. Jak: *Metall. Mater. Trans. B*, 2012, vol. 43, pp. 27–38.
46. T. Hidayat, P.C. Hayes, and E. Jak: *Metall. Mater. Trans. B*, 2012, vol. 43, pp. 14–26.